UNIVERSITY OF GHANA

COLLEGE OF BASIC AND APPLIED SCIENCE

FABRICATION AND CHARACTERISATION OF BIODEGRADABLE POLYMER COMPOSITES FOR PACKAGING APPLICATIONS.

BY

JOSHUA ASANTE TUAH

(10637867)

THIS THESIS/DISSERTATION IS SUBMITTED TO THE UNIVERSITY OF GHANA, LEGON IN PARTIAL FULFILMENT OF THE REQUIREMENT FOR THE AWARD OF MPHIL MATERIALS SCIENCE AND ENGINEERING DEGREE

DEPARTMENT OF MATERIALS SCIENCE AND ENGINEERING

2019

UNIVERSITY OF GHANA

COLLEGE OF BASIC AND APPLIED SCIENCE

FABRICATION AND CHARACTERISATION OF BIODEGRADABLE POLYMER COMPOSITES FOR PACKAGING APPLICATIONS.

BY

JOSHUA ASANTE TUAH

(10637867)

THIS THESIS/DISSERTATION IS SUBMITTED TO THE UNIVERSITY OF GHANA, LEGON IN PARTIAL FULFILMENT OF THE REQUIREMENT FOR THE AWARD OF MPHIL MATERIALS SCIENCE AND ENGINEERING DEGREE

DEPARTMENT OF MATERIALS SCIENCE AND ENGINEERING

2019

DECLARATION

Candidate's Declaration

I hereby declare that this MPhil thesis which is the result of my own original research under strict supervision was prepared in accordance with the University of Ghana's academic regulations and that no part of it has been presented for another degree in this University or elsewhere.

Candidate's name: Joshua Asante Tuah

Signature:…… Date:……

Supervisor's Declaration

We hereby declare that the preparation and presentation of this MPhil thesis were supervised in accordance with the guidelines on supervision of MPhil thesis laid down by the University of Ghana.

Supervisor: Dr. Benjamin Agyei-Tuffour

Signature:…… …… Date:…14th June, 2019……

Co-Supervisor: Dr. Abu Yaya

Signature:…… Date:……

Head of Department's Declaration

I hereby declare that this MPhil thesis has been prepared, supervised and accepted in accordance with the guidelines on the MPhil thesis laid down by the University of Ghana

Head of Departments: Dr. Lucas Nana Wiredu Damoah

Signature: …… Date: ……..

ABSTRACT

Environmental pollution by non-biodegradable plastics, gradual reduction and increase in cost of petroleum products used have affected lives over the years. With people using different kinds of packaging, it has a part of human daily living. Therefore, it is very important to find lasting and sustainable ways of producing and managing the wastes generated by these plastics. In this work, starch based biocomposites are fabricated and characterised to access its opportunities to replace petroleum based plastics. The modifiers that were considered for reinforcement purposes were nanokaolin and cellulose nanofibers extracted from rice husk.

Stress strain diagrams were obtained from the tensile test method. From the stress-strain curve, the yield strength, ultimate tensile strength and the fracture strength of the various biocomposites were determined. The material that was shown to give good response to the tensile load in terms of the yield, and fracture was seen to be TPS-0.2kaolin biocomposite. This can be associated to goof interphase reaction between the nanoclay and the starch polymer at nanoclay volume fraction of 0.2. Water vapour transmission test also pointed to biocomposites of cellulose volume fraction 0.5 as the appropriate material with best water vapour barrier properties. This is associated to the reason that at cellulose volume fraction of 0.5, the cellulose whiskers are very compact and dispersed all over the biocomposites and hence restricts the escape of water in the form of gas from the film. This confirms the reason why the strength of the TPS-cellulose biocomposite is higher at volume fraction of 0.5.

FTIR analysis was conducted for thermoplastic starch (TPS) only, TPS-nanokaolin biocomposites and TPS-cellulose biocomposites. The spectra for TPS only pointed to the presence of OH-stretching due to the water used during fabrication, CH- bending and some C-C bonds. The spectra for TPS-nanokaolin was similar to that of thermoplastic starch, however, there was a new band showing the presence of Si-O-C bonds due to the chemical reaction of

the nanokaolin (alumino-silicate) to the water and starch. The spectra for TPS-cellulose showed the presence of OH- stretching bond, CH-bends, C-C bonds.

The FTIR results showed the presence of water and other chemiclas that affect the strength of the biocomposites prepared. This gives an idea of what to expect for the results of the mechanical properties.

Scanning Electron Microscope micrographs shows that nanokaolin particles were successfully introduced into the TPS matrix and it was uniformly dispersed in TPS-nanokaolin nanocomposite films at optimum nanokaolin volume fractions. The micrographs for TPS-cellulose biocomposites showed that cellulose fiber was successfully introduced into the TPS matrix but the fibers were not uniformly distributed.

Energy Dispersive X-ray spectroscopy (EDX) also gave the representation of elements present in the TPS-nanokaolin and TPS-cellulose biocomposites. This analysis technique confirmed the presence of Al, Si, O (known to be present in nanokaolin), and C (known to be present in starch and glycerol) in TPS-nanokaolin biocomposites. Also, the presence of O, C, Ca, Si, Na was confirmed in TPS-cellulose biocomposites. With C, O representing the elements in cellulose, Ca and Si known to be elements which are present in rice husk. The Na was recorded as a traces left after the extraction process.

Biocomposites prepared from starch, glycerol, and nanokaolin composites are seen to show broad peaks which is known for semi-crystalline materials. However, the degree of crystallinity increases as the volume fraction of nanokaolin increases.

DEDICATION

This work is dedicated to my parents, Pastor Asante Botwe and Mrs. Joyce Asante for their unwavering support throughout my education.

ACKNOWLEDGEMENTS

First of all, I thank the Lord Almighty for the gift of life and good health throughout my study. A special thanks also go to my Supervisors, Dr. Benjamin Agyei-Tuffour and Dr. Abu Yaya for their advice, and directions throughout this work.

I will also like to thank, Dr. Emmanuel Nyankson, Dr. David Dodoo-Arhin, Dr. Ebenezer Annan, Dr. Lucas N. W. Damoah, Dr. Johnson Efavi and Dr. Yaw Delali Bensah, Prof. B. Onwona-Agyeman, Mrs. Gloria P. Manu and Mr. Essien for all their advice and encouragements during my time of the study.

Table of contents

LIST OF TABLES

LIST OF FIGURES

LIST OF ABBREVIATIONS

ABBREVIATIONS	FULL MEANING
Vf	Volume fraction
PP	Polypropylene
PS	Polystyrene
PE	Polyethylene
PTFE	Poly-Tetrafluoro ethylene
IR	Infrared
XRD	X-ray Diffraction
FTIR	Fourier Transform Infrared
SEM	Scanning Electron Microscopy
UTS	Ultimate Tensile Strength
TPS	Thermoplastic Starch
RH	Rice Husk
rpm	revolutions per minute
EDX	Energy Dispersive X-ray spectroscopy
WVTR	Water vapour transmission rate

CHAPTER ONE

1.0. INTRODUCTION

1.1 Background

The increased demands for products, be it consumable or non-consumable has aroused the interests in packaging materials. Different materials including glass, paper boards, plastics and metals are the common packaging materials used in the industry. Packages are marketing strategies which enable customers to know information such as name, brand, colour, identity, content of product etc. Aside these marketing strategies, packages are to serve the required purpose for which they are used.

These packaging materials serves as an enclosure to the product, prevents attacks from environment on the product, enables easy handling and transportation of products, improves the aesthetic value of the product, communicates the details about the product and also maintain the integrity of the product.

Increase in the quantity of packages used in our everyday living has had an impact on the amount of waste that is generated daily and is becoming a nuisance in the environment. This is as a result of the waste not been biodegradable and hence accumulating in landfills and hence encroaching on settlement, clogging water ways and causing floods and threatens wildlife. According to the state of environment report in 2017, solid waste generation in Ghana is estimated at 13,500 tonnes per day and out of this about 29% made of household waste is discarded into gutters, open fields, streets, etc. These are the sources of pollution which is negatively impacting human health, water and land quality. The composition of plastics and rubber waste in the country is about 18%. This quantity is huge enough to cause trouble many ways [15].

In the quest to find a solution to this nuisance caused by the non-biodegradable polymers, some individuals have resorted to burning the plastic waste. However, this is also harmful to the health of human. This is because plastics contain toxic chemicals such as phthalates, cadmium, ethylene dichloride, vinyl chloride etc. which is capable of leaching out of plastics and absorbed in the blood stream [24].

The non-biodegradability of these packaging materials have aroused great environmental fury from the consumers, environmental advocates, civil societies and the media and therefore the urgent need for a reliable and sustainable packaging materials to replace the plastics and glass cannot be overemphasized.

Biodegradable plastics are stipulated to be the replacement for the non-biodegradable petroleum plastics that have been used for packaging applications over the years. Extensive research is being done in this field to find sustainable results and remedies to their limitations. Examples of biodegradable polymers that have found application in packaging are starch, chitosan, poly(lactic acid), polycaprolactone, polyhroxybutyrate, etc. However, starch is known to be readily available and of low cost.

1.2 Justification

Environmentalists keep fighting against the single use of plastic material which they suggest is the cause to the nuisance we see in the environment. However, it will not be possible to use one packaging materials for more than once due to the different sizes and types of products available. It is possible rather, to produce biodegradable plastic packages that will be used once and collected to a common point where degradation takes place.

Consumers, at the news of the introduction of biodegradable packaging materials also have raised concerns that these biodegradable packages may not be fit mechanically to protect the products. However, biodegradable polymers can be modified with nano materials such as clays,

etc. to form biocomposites which is fit mechanically to protect the product. Hence this research seeks to prepare biocomposites from natural materials such as starch, nanoclay and cellulose nanofibers obtained from coconut fibers, ginger, rice husk etc. these materials are readily available and its usefulness is not well exploited.

1.3 Problem Statement

Packaging materials are mostly made of plastics. The disposal of these plastics after their use and lifetime has caused a nuisance in the environment. We see these plastics in our water bodies (sea, river, lagoons, dams etc.), on the streets, in gardens and so many places. These plastics are directly affecting wildlife by chocking fishes as well as killing birds. These plastics also affect the plant life by covering the plants and blocking the sunlight that aids the plants in photosynthesis and hence killing it. The accumulation of these plastics on the landfill sites also takes so much space because they take too long (about 50 to 1000 years) to degrade.

The gutters get chocked with these plastics. At the incidence of a heavy rain, the water has no path to travel through hence floods occur which destroys a lot of properties and takes peoples life.

1.4 Research Question and Hypothesis

1.4.1 Research Question

i. Can nanokaolin and cellulose extracted from agro waste such as rice husk be an appropriate modifier for starch based biocomposites?

ii. Does the content of the clay or cellulose affect the properties and morphology of the biocomposite?

iii. Is the biocomposite prepared from starch and clay or cellulose suitable to be used for packaging?

iv. Does the morphology of the biocomposite affect its packaging application properties?

1.4.2 Research Hypothesis

The research was guided by the following research statement which was be tested by undergoing the various objectives and purpose of the project.

The research hypothesis states that, “the increase in the volume fraction of nanoclays and cellulose nanofibers in the biocomposites can affect their mechanical, microstructural and thermal characteristics of the biodegradable composites”.

1.5 Purpose and objectives

The purpose of this project is to prepare and characterize biodegradable composites for packaging applications.

To achieve the stated purpose, the following objectives were carried out:

- To prepare starch-based composites using clays and cellulose whiskers as reinforcements.
- To determine the microstructural, mechanical and thermal properties of the biocomposites.
- To perform analytical and numerical modelling to validate the experimental results.

1.6. Scope and Limitation

1.6.1. Scope

This research focused on fabricating and characterising biocomposites from readily available natural agro materials, agro waste and nanokaolin. The research is limited to these materials due to its readily availability and cost. And the primary focus of application is food packaging.

1.6.2. Limitation

The study was limited in the following ways:

i. The biocomposites were only tested for water vapour transmission rate. Leaving out the gas vapour transmission rate due to inaccessibility to the equipment.

ii. The melt flow index of the starch thermoplastic was not considered in this study.

iii. The individual properties of the cellulose nanofiber and clay were not considered in this study.

iv. The analytical and modelling aspect was considered only for the mode of failure with images to show for it.

CHAPTER TWO

2.0. LITERATURE REVIEW

This chapter reviews most theoretical principles that are available for this work. It focusses on the history, types, applications, methods and properties of composites and biocomposites, packaging materials and systems available, introduction to finite element analysis using abaqus CAE used for modelling the numerical aspect of the research. Details of the modelling and steps followed, the types of modifications that are used in similar works are all reported in this chapter.

2.1 Composites

Composite is a naturally occurring or man-made material made up of two or more phases [71]. The different phases present in every composite material can be classified as matrix or reinforcements. The matrix serves as the host material in every composite with certain properties which can be modified or reinforced using the second phase which is the reinforcement.

Composites can be classified by the mode of existence or production. The two most common classes of composites are natural composites and artificial (man-made) composites. Natural composites are those that exist by nature. Examples are wood and bone. Wood consists of cellulose fibers surrounded by lignin which serves as the matrix. The cellulose fibers make it possible for wood to bend whiles lignin makes wood stiff. Man-made composites are those that are designed and produced by combining two or more of engineering material. Mostly they are composed of ceramic phases, polymer phases, metal phases. Examples of man-made composites are concrete, glass fiber reinforced polymer (GFRP), etc.

Materials that are used as reinforcements in composites have different morphologies. These include, particles, whiskers, fibers. Composites designed with whisker morphologies are mostly discontinuous in all directions unlike particulate morphologies which are uniform in all directions.

Composites designed with fiber morphologies can be designed to support load in different directions. The directions are unidirectional, or bidirectional. For unidirectional, loading can be applied perpendicular or parallel to the orientation of the fibers.

Composites are designed with the aid of the rule of mixtures. This theory can be used to give an estimation of the composite mechanical and physical properties in different directions [71].

2.1.1 Fiber reinforced composites

Mechanical properties of fiber reinforced composites can be estimated in different direction. The two major directions that are considered and is mostly dominant in composites are the transverse and longitudinal directions.

The rule of mixtures for composites which has fibers oriented longitudinally to the direction of the load applied is known to be constant strain, whiles that with the fibers oriented transversely to the direction of the load applied is known to be constant stress.

Considering the constant strain theory (from equation 2.1 to 2.12), the matrix and fiber strains must be equal (equation 2.11) to enable the load applied on the composite to be the sum of the load on the matrix and fiber (equation 2.1). The derivation if the composite stress equation is shown from equations 2.1 to 2.6. It starts with the load expressions shown in equation 2.1. Equations 2.2, 2.3 and 2.4 were used to obtained equation 2.7. The volume fraction equations used is shown in equation 2.5 and 2.6.

$$P_C = P_m + P_f \quad \text{.....2.1}$$

$\sigma = \frac{P}{A}$; P = σA …….....2.2

$\sigma_c A_c = \sigma_m A_m + \sigma_f A_f$ ……...2.3

$\sigma_c = \frac{\sigma_m A_m}{A_c} + \frac{\sigma_f A_f}{A_c}$ ……...2.4

$V_m = \frac{A_m}{A_c}$ ……2.5

$V_f = \frac{A_f}{A_c}$ ……2.6

$\sigma_c = \sigma_m V_m + \sigma_f V_f$ ……2.7

Likewise, from the Hooke's law (equation 2.8), the equation to estimate modulus of elasticity for the composites (equation 2.12) can be derived by operating on the composite strength expression (equation 2.9), and the strain (equation 2.11).

σ = Eε …….....2.8

$\sigma_c = \sigma_m V_m + \sigma_f V_f$ ……...2.9

$E_c \varepsilon_c = E_m \varepsilon_m V_m + E_f \varepsilon_f V_m$ …….....2.10

$\varepsilon_c = \varepsilon_m = \varepsilon_f$ …….....2.11

$E_c = E_m V_m + E_f V_m$ ……...2.12

Considering constant stress theory, the stress applied to the composite is the same as that applied to matrix and reinforcement (equation 2.24). In this case, the displacement in the composite (equation 2.13) can be estimated by a sum of the displacement in matrix and displacement in fiber.

$\Delta l_c = \Delta l_m + \Delta l_f$ ……...2.13

From the engineering strain (equation 2.14 and 2.15), which is the ratio of displacement to original length,

$\varepsilon = \frac{\Delta l}{l}$ …… 2.14

$\Delta l = \varepsilon l$ …… 2.15

$\varepsilon_c l_c = \varepsilon_m l_m + \varepsilon_f l_f$…… 2.16

$\varepsilon_c = \varepsilon_m(\frac{l_m}{l_c}) + \varepsilon_f(\frac{l_f}{l_c})$…… 2.17

The ratio of lengths gives the volume fraction (equation 2.18, 2.19 and 2.20).

$V_m = \frac{l_m}{l_c}$ …… 2.18

$V_f = \frac{l_f}{l_c}$ …… 2.19

$\varepsilon_c = \varepsilon_m V_m + \varepsilon_f V_f$ …… 2.20

From Hooks law (equation 2.21),

σ = Eε ……..... 2.21

$\varepsilon = \frac{\sigma}{E}$…….. 2.22

$\frac{\sigma_c}{E_c} = \frac{\sigma_m}{E_m} V_m + \frac{\sigma_f}{E_f} V_f$ ……..... 2.23

For constant stress,

$\sigma_c = \sigma_m = \sigma_f$…… 2.24

$\frac{1}{E_c} = \frac{1}{E_m} V_m + \frac{1}{E_f} V_f$ …… 2.25

$E_c = \frac{E_m E_f}{E_m V_f + E_f V_m}$ …….. 2.26

Figure 2.1 [71] below show the diagram for constant strain and figure 2.2 [71] shows that for constant stress theories.

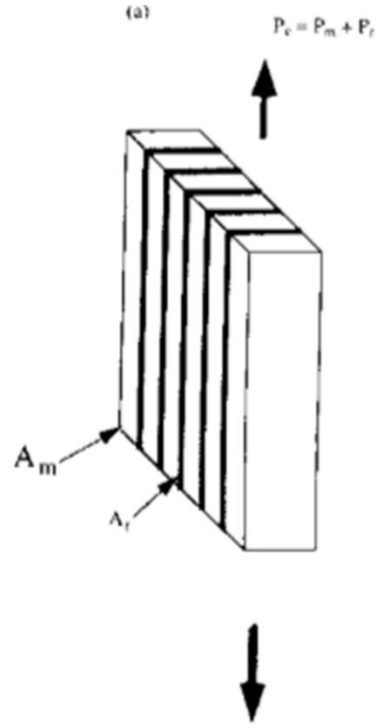

Figure 2. 1 Schematic for loading configurations for constant strain theory.

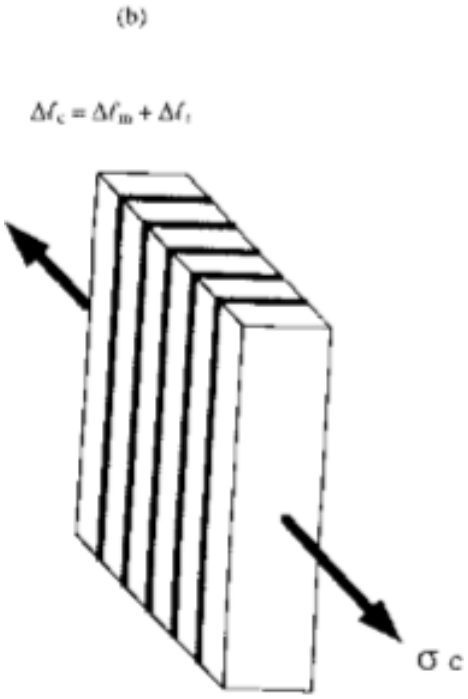

Figure 2.2 Schematic for loading configurations for constant stress theory

With the above configurations, we can then estimate the modulus and strength of composites depending on the way the fibers are aligned to the load to be applied [71].

2.1.2 Particulate reinforced composites

Particulate reinforced composites are mostly cheap and widely used in varying applications. Most particulates used as reinforcements in these kinds of composites are harder and stiffer than the matrix. These kind of composites can further be classified into ones with large particles as reinforcement and others with dispersions as reinforcements.

Dispersion phase particles are mostly of sizes 10-100 nm whiles large particulate reinforcements are mostly of sizes 10-100 μm. The large particulate reinforcements act by restricting the movement of the matrix when bonded well with the matrix. These particulates have different geometries, but should be approximately the same dimension in all direction. Also, the volume fraction of the particulate reinforcement and matrix phases influences the behavior and mechanical properties [69]. The examples of large particle reinforcement composites are concrete, cermets, reinforced rubber, etc.

The rule of mixtures for fiber reinforced composites was represented with the constant strain theory and the constant stress theory. For particulate reinforced composites, the rule of mixtures equations predict that the elastic modulus should fall between the upper bound (constant strain) and lower bound (constant stress) as shown in figure 2.3.

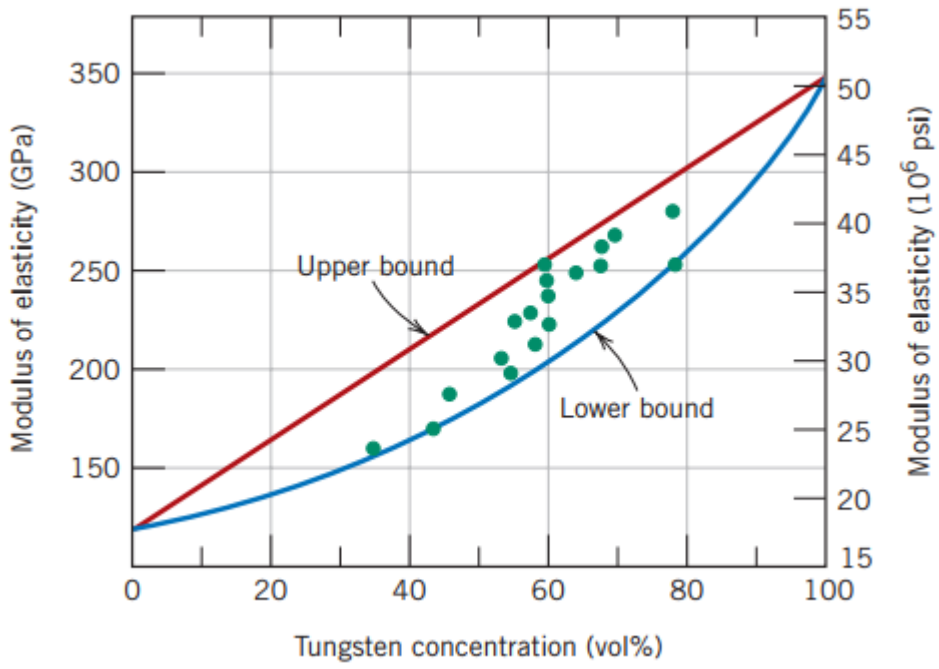

Figure 2.3 Representation of elastic modulus for particulate composites [69]

2.2 Biocomposites

Biocomposite are a group of composites that is composed of a biodegradable polymer as the matrix and a biodegradable natural fiber as the reinforcement. Polylactic acid, Polyvinyl acetate, Polycaprolactone, Starch, Chitosan, Egg white, etc are all examples of biodegradable polymers that are used as the matrix material in the fabrication of biocomposites. In such composites, the fibers are mostly natural fibers such as hemp, cotton, ramie, kenaf, coir, flax, jute, etc. According to Affo et.al, combining two bioplastics to form a composite helps to improve the properties [68].

These kinds of composites have received much interest and attention due to the availability and sustainability of the materials involved. This have aroused much researches to find a more sustainable combination of matrix and fiber.

From an environmentalist point of view, these biocomposites pose huge benefits to the environment. These benefits include low energy required for fabrication, low CO_2 release,

reduces the depletion of petroleum based resources, positive impact on agriculture and reduce environmental pollution [58].

2.3 Fibers

Fibers are materials with thin diameters and are normally separate from each other. Fibers can be likened to threads [69]. Generally, fiber diameters can be classified from super fine to very course. For instance, wool fibers have diameters of about 16- 40 microns, glass fibers have diameters between 1-5 micrometers and that of carbon fibers is 3-14 micrometers.

For a composite material to be considered as one with high strength, the fibers must be oriented well. High strength properties are normally achieved when the fiber can effectively carry the load which has been transferred by the matrix and also when there is interactive bond existing between the fiber and the matrix [20]. Fibers are basically classified into two forms as shown in figure 2.4, they are natural fibers and man-made fibers

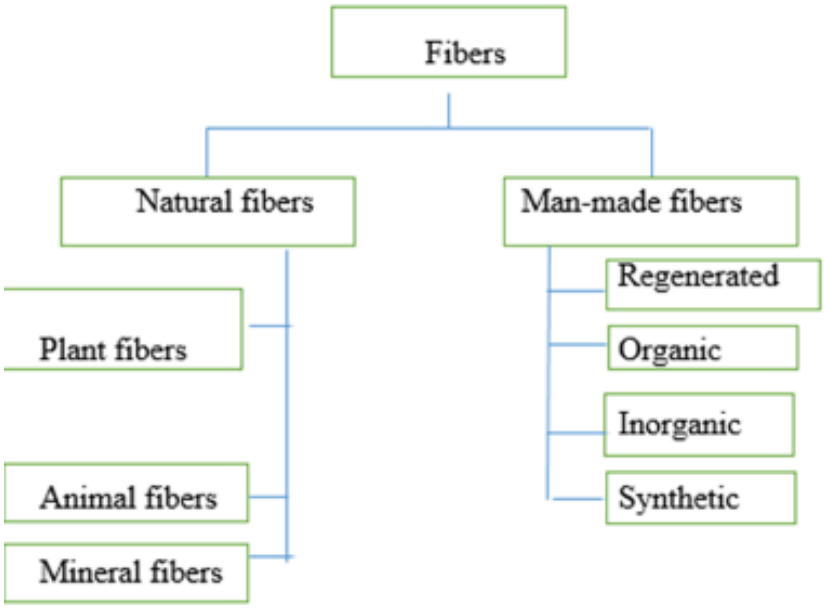

Figure 2.4. Schematic diagram for classifications of fiber

Generally, fibers can be used in various forms and they include; making of clothing in the textile industry, making of paper, making of furniture and making of medical devices such as artificial arteries. They are also used as reinforcements in concrete, automobile, bath fixtures

and sports equipment [18]. In all these applications, the fibers add some properties to the component to which it were added.

2.3.1 Natural Fibers

Natural fibers have their form as threadlike materials. From figure 2.4 shown above, materials that are grouped as natural fibers include plant fibers, animal fibers and mineral fibers and these classifications are based on their origin. Observing a natural fiber with the eye, it is realized that it normally has long length and negligible diameters. Examples of natural fibers are cotton, flax, jute, silk, sheep wool, coconut fiber, sisal, bamboo and asbestos. Natural fibers are normally used because they are generally cheap, renewable, hydrophilic, strong and less dense. Animal fibers are mostly obtained from the skin or the fur of animals. Examples are horse hair, sheep wool and goat hair. Animal fibers are used for making footwear and for aesthetic purposes. In composites such as ceramic based concrete, animal fibers can be used as reinforcements to increase the properties and arrest cracks created in the composites.

In processing animal fibers, firstly they are cut into pieces then washed in various containers of hot soapy water to remove the wax, grease and impurities the fiber might have accumulated. After washing them, they are dried under sun and passed through different rolls of different diameter to form thin webs of fiber. Afterwards, the fibers are separated individually for use.

Plant fibers are obtained from plant stem and contain cellulose. They can be seed-hair, leaf and husk. Examples of plant fibers are cotton, flax, jute and coir fiber. Some applications of plant fibers are; for making clothing in the textile industry, for production of thermo-insulating materials, for the production of ropes, for making upholstery, for making mats, for making of bank note, for paper production and for making brushes and life vests [43]. Cotton is used in the textile industry for making clothes due to its fine feel and its ability to allow free flow of fluids. On the other hand, bamboo is used for making thermo-insulating materials based on its low thermal conductivity. For the production of ropes, upholstery and mats, jute fibers as well

as coir fibers are preferred as a result of its ability to stretch. In making bank notes, plant fibers with short lengths are used. Recently, plant fibers are being researched into to be applied as reinforcements in biocomposites due to their availability, cost and strength.

In processing plant fibers, the plant material after harvesting is placed in water or kept wet. This is done to allow the bacteria to digest away most of the plant tissues. Bacteria is formed from reacting the plant fiber with the water. The material when taken out of the water is passed through a spinneret to segregate them into fibers. The fibers obtained are beaten and treated with chemical to separate the lignin from the cellulosic fibers.

Mineral fibers are derived from natural mineral sources. They are usually known to be poor conductors of heat, electricity and sound. In addition to their properties are: resistance to high temperatures because they have large values of magnesium oxide concentration, high durability and insolubility in water. An example of mineral fiber is asbestos.

Mineral fibers are used for fireproof clothing, brake linings, gaskets, industrial packing, electrical windings, insulations, and soundproofing materials [30].

Most mineral fibers are produced from slag or a mixture of slag and rock. The mineral feed together with coke is mixed in a ratio of 5-6 part of mineral to 1 part of coke and then loaded alternatingly in a cupola. The mineral component changes phase to the molten state at a temperature of about 1500°C as the coke is burned. The molten mineral charge exits the bottom of the cupola and falls unto a fiberization device which forms long fibrous tails of the mineral [36].

2.3.2 Man-Made Fibers

Man-made fibers do not occur naturally but are obtained by some processes such as rolling and/or joining two or more materials together. Man-made fibers are the most used fibers amongst all the classes of fibers and this is due to its ease of processing and it been easily

recycled. Taking steel fibers for instance, after it is readily available in the earth crust. The types of man-made fibers are regenerated, organic and inorganic.

Regenerated man-made fibers are obtained by processing a natural polymer which is a long chain of monomer units occurring naturally. Among some of its properties are: its relative fast drying, its availability in a wide range of colours.

Another form of man-made fibers are inorganic fibers which are made from materials such as glass, metal, carbon or ceramic. Examples of this type of man-made fibers are steel fibers, carbon fibers and glass fibers.

2.4 Polymers

Polymers are molecules with long chains that are come together from many different smaller molecules called monomers [11]. A repetition of these smaller molecules in long chains, sometimes with branching or cross-linking between chains is termed as a polymer.

To form the polymer chains, monomer molecules are reacted together in a chemical reaction known as polymerization. The monomers that react together may be alike or may be from two or three different compounds.

There are two sources of polymer. These are the synthetic sources and the natural sources. To differentiate between the two sources, the mode of formation or derivation is used. Synthetic polymers also known as synthetic plastics are basically derived from petroleum products. They are most times the by-product of petroleum production. Natural polymers on the other hand are derived from plants and natural activities.

2.4.1 Synthetic Plastics

Synthetic plastics are those which are derived from petroleum oil. They can be either biodegradable with examples like polycaprolactone(PCL), polylactic acid (PLA), etc or non-

biodegradable such as nylon, polyethylene, polyester, Teflon, epoxy, etc. Biodegradable polymers have the tendency of been destroyed or degraded when enzymes act on them or when heat is applied to it. This makes it difficult to recycle. However, synthetic polymers that are not biodegradable will take about 50 to 1000 years to degrade. The most used form of destroying these kinds of polymers is to subject them to high temperature at which the polymer branches will be broken and the material is destroyed. At the application of heat, harmful gasses such as carbon is released into the atmosphere which is detrimental to human health. Synthetic polymers that are not biodegradable have various effects on the ecosystem. Synthetic polymers are mostly used in food packaging, general packaging and also for making appliances. For this reason, there is landfill accumulation, and pollution in our environment. This occurs because the polymers are not biodegradable [4].

2.4.2 Natural Polymers

Natural Polymers are those which can be found in nature and can be extracted from plants, and other natural sources. These types of polymers are mostly water-based. Natural Polymers includes polysaccharides (sugar polymers), polypeptides (silk, keratin, hair). Examples of natural sources of polymer are starch, cellulose, chitin, proteins.

Natural polymers are mostly known to be thermoplastic. This means, they have the tendency of been dissociated or degraded when heat is applied to it after it has been moulded.

2.4.3 Biodegradable Polymers

Biodegradable polymers can be defined as polymers that happens to change in chemical structure when there is an action of enzymes, which brings about significant loss in physical and mechanical properties as defined by the America Society for Testing of Materials (ASTM) and the International Standards Organisation (ISO). Research on biodegradable plastics have increased over the years which reports that biodegradable polymers can be obtain

biodegradable polymers are produced from renewable natural sources such as polysaccharides (cellulose, starch, chitin), lipids (oils), proteins (gelatin and gluten), plant/microbial polyesters or synthesized from renewable sources such as polyesters produced from bio-derived monomers like polylactic acid from starch [37]. They are polymers that is mostly attacked by microbes. Microbe attach ends up in mineralisation, photodegradation, oxidation and hydrolysis of the product [3]. Biodegradable plastics have many deficiencies compared to petroleum based plastics, and these deficiencies limit its use in the food packaging industry [8]. However, these biodegradable plastics have been modified and their properties are now close to that of the petroleum based plastics [66].

2.4.3.1 Starch-based Plastics

Starch, one of the most abundant biomolecule on earth just as cellulose and the major carbohydrate reserve in plant tubers and seed endosperm (maize). Starch consists of amylose (normally 20-30%) and amylopectin (normally 70-80%).

Starch is very useful in diverse ways and Industries and has potential to be used as a biodegradable plastic because it is abundant and cheap [35]. The sources of starch include cassava, maize/corn, potato, wheat, rice.

Cassava is among the most produced crops in Ghana and it is as well consumed as such because it is cheap. Cassava starch is the powder obtained from grated cassava. During preparation of the cassava starch, the cassava is graded into powders, mixed with water and allowed to settle after sometime, then the water is filtered out, leaving the starch at the base of the container.

Cassava starch is very hygroscopic and easily absorbs moisture from the surrounding air hence makes it very appropriate when to be used for food packaging applications.

Tapioca starch (as known by many) can be procured from the local market. To be used for preparing packaging films, it has to be processed well [52]. Despite its usefulness and availability, starch is a hydrophilic materials and this property of starch is responsible for its incompatibility with most polymers that are not able to react with water (hydrophobic). Starch on its own is not a thermoplastic material but when plasticizers are added and stirred in the presence of heat, it is able to melt and flow. Thermoplastic starch is the end product of applying mechanical force and plasticizers such as glycerol and water [28]. To obtain the thermoplastic starch, mechanical energy (in the form of stirring) and thermal energy (in the form of heating) is required [17].

According to Alves et al, cassava starch films are odourless, tasteless and colourless. These edible films provide good flexibility. The drawback of cassava starch film is their rather low tensile strength. To improve upon this property, cellulose nanofibers can be introduced into the starch [67].

Nanoclay can also be used as a modification to cater for the draw backs of cassava starch films. These are mostly layered silicates with thickness being around the nanometric region and its diameter is normally around 50–200 nm [42].

Advantages of nanoclays that encourage its use as reinforcing fillers include their wide availability and lower cost. For these advantages, they are mostly used to prepare nanocomposites of polymer based composites with starch as t base matrix material being an example [63]. Research shows that incorporating nanoclays into polymeric matrixes has the chances of enhancing the mechanical, physical and barrier properties of polymers. Montmorillonite, kaolinite and saponite are examples of nanoclays used as fillers to modify the properties of polymers. In researches where these nanoclyas are used to blend and modify the polymers to form nanocomposites, it is reported that there is an improvement in mechanical

properties such as strength, elastic modulus, toughness and physical properties such as barrier and flame retardant properties [40].

2.5 Packaging materials

The history of packages shows that, the reason why packages were developed or came into existence was to provide covering and protection to the product. Products at that time were then placed in reliable and readily available packages made from materials usually taken from natural resources such as wood pulp, or textile. Out of wood pulp, paper and cardboard were produced. Also, out of textiles, flour sacks were produced. These packages gave the consumers the comfort to enjoy the contents of the packages from their various homes. In those periods, the most common material that were used for packages were paper and glass, hence they took the role of packages to mean a protection on the way home. This meant that packages were made to last for a shorter period.

To inculcate protection at home and also for a longer period of time, technology came to improve manufacturing parameters at around the eighteenth century when manufacturers of products that require packages were made to develop more strong and resilient packages that could allow the products to be easily transported from the factory to the retail and wholesale shops and later on the consumers or customers. About 200 year ago, manufacturers and producers of products were not informed on the techniques to improve shelf-life of the product. This was because of the limited or no information gathered by researchers in the field of packaging. This gave manufacturers very little variety of materials to choose from. However, plastic materials were fully discovered to be potential candidates in packaging applications later in the 1860s [21].

The breakthrough came as a result of altering hard rubber. Later, inventions of the various information and techniques to prepare plastics were developed and this began with the

preparation of celluloids and followed by synthetic plastics. Example of these synthetic plastics that were prepared after the breakthrough is polyvinyl chloride (PVC), prepared by Nobel prize winner Herman Staudinger after he made a breakthrough during his dedication to study polymer science. PVC is recently used in huge quantities in modern packaging materials. Another scientist (a DuPont chemist) in the 1940s did a further study of synthetic polymers and discovered that synthesised polyethylene terephthalate (commonly known as PET). PET has since then been used for manufacturing plastic bottles even until today [51].

Another form of material that as packages mostly in the brewery is metals. Most of the metals used are tins and steels coated with chromium. These metal packages back then during the war were used as weapons in the Europe after they have used it in serving their beverages [55] and sometimes soup and preserved fruits [21].

2.5.1 Functions of package materials

Every author and textbooks will have their own different descriptions for the functions of packages. However, they may be some similarity between the structures. The functions of packages include containment, protection, preservation, convenience, information, communication, promotion, environmental responsibility and other.

Containments is the ability of the package give covering to the product and prevent it from spilling and being lost. This begins from the manufacturer, where packaging is done through transportation to the end user, the customer. If the containment for liquids and chemicals in particular are not properly done, it can be detrimental to the environment and people. Every package has a point or points that are sensitive. These points, when not handled well can affect the containment and the product.

Hence manufacturers and producers are very particular in undergoing stringent protocols which includes testing the package to ensure that the products are properly contained [65].

Transportation of products such as tools, clothes or food to various homes from the market is one thing that cannot be overlooked. In the period of transportation, the product must be protected to prevent it from alterations such as environmental attack which includes the air, dust, vibrations weather conditions, or animals. The protection that packages gives to products, helps to prevent all outside forces and variables from interfering with the product inside the package. Particular products also require that specific temperatures and humidity levels are maintained in order to be preserved. Therefore, packages should be able to withstand the temperature and humidity levels of the product being packaged. To be able to protect the product sufficiently, it is necessary to understand the characteristics as well as the potential hazards that goes with these required characteristics [65].

The preservation function is not applied to all the products that require packages, it is mostly taken into consideration when dealing with raw food products, pharmaceuticals and other perishable products. In order to help keep the product under stringent and controlled environment to achieve the safety of the product for consumers, preservation is done. This makes it safe and remains useable for very long periods. To be able to preserve the product and keep it very safe, it will be very important to understand the mechanism of spoilage of the product being packaged. In this stage, the package must address the potential cause(s) of product spoilage. Most times, preservation is done and very necessary for products that need to maintain certain levels of oxygen, moisture, volatiles or their sensitiveness to light [2].

With bases being on the fact that a package is a tool which to maintain the products in certain desired conditions, it should also be very convenient during transportation until it reaches the end user (customer or consumer).

Another function of packages which is most times considered by customers or consumers, is the convenience function. The convenience function tends to deal with the size and the mode of disposal of the packaging. One example is the decision a customer takes to choose between

buying a drink packaged in tin cans, which once opened cannot be left ajar until the content is fully consumed or a drink in a plastic bottle which can be covered intermittently until the whole product is consumed. This example tends to confirm that different packages comes with different ways of using them [29].

Packages also gives out information which include data to enable tracking, the information about the product such as name and content, marketing and brand information. Bar codes are the most used amongst other tracking information used on packages. These bar codes are normally not targeted to consumers but they are placed there to communicate the metadata of the product to authorities to verify for originality. In order to read these metadata, scanners or detectors are needed. This information included the manufacturer, basic description, dimension of package, and data of the product that are not likely to change over some period [38].

Recently, society have become intensively interested about products, its content and materials or ingredients used to make the product. Hence smart phones are now equipped with applications that can be used to read the bar codes. The growing of technology therefore has helped for easy scrutiny of products to prevent any replica of product from being sent to the market and also to enable consumers the access to more data about the products they seek to purchase [65].

There is a high demand for different kinds of products as the years go by and this has affected the environment. The effects of the high demand of product on the environment is in the form of litter and waste from packages. This has triggered the creation of citizen's initiatives to decrease the amount of waste generated [45].

Another effect of the high demand on product which require packages is afforestation. Packages that are produced from natural resources (trees in particular) such as paper are the causes of the afforestation. Likewise, the use of non-renewable resources like steel products,

petroleum also has strong influences on habitats and energy consumed as a results of the mining and material preparations which emits harmful gases and takes more energy.

According to Aaron, “some states, such as California, Colorado and Texas have passed a law which is being regulated as bans plastic bag”. This regulation was done in 2014. Where in California, people were prohibited to use plastic bags once in the supermarkets [32]. Authorities in Kenya also took a similar but much harsher approach, where they considered the selling, producing and use of plastic bags as a criminal act and punished culprits with the payment of huge fines or serving jail times [22]. Likewise, the European commission also took actions by setting goals for the consumption or use of plastics to an average of 40 bags per person in a whole year by 2025. Their decision was based on study conducted in 2011 about the use of carrier bags in individual EU countries [14]. In Finland and Denmark, the average yearly consumption or use of single-use bags ranges from 4 bags and that of Czech Republic is 297 bags [16].

Before every design of a packaging material is considered capable to pass its function test, it must have endured all basic properties in the ambient, human, and physical environment. These functions must be taken into consideration during the material selection and designing phase of manufacturing of the packages by the companies. Even though the functions of these packages must be considered during manufacturing, the business objectives which include cost, availability, brand image, marketing. These must be considered together with each other and not solely during manufacturing [65].

2.5.2 Packaging systems available

Packages can be categorized into four groups. These groups are primary packaging, secondary packaging, distribution or tertiary packaging, and unit load.

The first-level package that deals directly with the product is referred to as the “primary package”. Primary packages come directly into contact with the product and the major function of these kind of packages is to preserve the product [72]. These kinds of packages must not contain toxic substances and also it must be compatible with the product. These kinds of packages are not supposed to cause any changes in the product’s attributes such as its colour, flavour and chemicals present.

Secondary packages are mostly made up of two or more primary packages. They protect the primary packages from getting damaged during transportation and storage. These kinds of packages are also most times used to prevent dirt and contaminants from affecting or contaminating the primary package [61].

Tertiary package, also known as shipping containers shipping containers normally contains a number of secondary and primary packages. It is most times referred to as the “distribution packages” [61].

Most times, a group of tertiary packages are put together to enable mechanical handling, shipping and storages. The assembly of these tertiary packages makes up a unit load which is most times transported or carried using trucks or fork-lifts or any similar equipment [61].

2.5.3 Materials for food packaging

Materials that have mostly been used for packaging includes plastics, paper, metal and glass. Taking plastics into consideration, they can be formed into different shapes using controlled heat and pressure at relatively low temperatures. The temperature involved in the processing of plastics is lower than that involved to produce metal and glass. This means that less amount of energy is conserved when producing plastics than when producing metal packages and glass packages. Every plastic has unique characteristics based on its chemical composition. Plastics

materials that are discussed are polyethylene, polypropylene, polystyrene, polyester and polyamides (PA or nylon).

Polyethylene (PE) commonly known as polybags is polymerized from ethylene and it is one of the plastic which is most commonly used for packaging. The general properties of PE include its flexibilities, efficient moisture control, resistance to oil and chemicals, efficient impact strength and inexpensive. Its cost makes it an economical choice where performance is suitable.

Polypropylene (PP) is polymerized from propylene gas, which is a relatively low-cost feedstock like ethylene [72]. PP also very efficient in chemical and grease resistance, possess good water vapour but poor gas barrier properties. The weakness of pp is shown in pp bags which cannot be retained for six months and hence makes it not suitable for long term storage [10].

Polystyrene (PS) is a linear addition polymer of styrene resulting in a benzene ring attached to every other carbon in the main polymer chain.it is mostly used in packaging food due to its aesthetic properties.

However, in a packaging application where extended shelf life is needed, PS cannot be a candidate because of it is not able to resist the passage of water vapour and gasses though its structures. Polystyrene foam is another form of PS that is mostly used in packaging applications for protecting appliances in boxes to prevent them from direct impact. It is also used in food packaging applications such as disposable coffee cups, meat and produce trays, egg cartons, etc.

Polyethylene terephthalate (PET) is commonly produced by the reaction of ethylene glycol and terephthalic acid. The properties of PET that has drawn interest in packaging applications include efficient mechanical properties, chemical resistance, light weight, reasonably high barrier properties. However, PET materials are not able to maintain its general shape in molten

state and it is very difficult to form and seal when it is in that state. One disadvantage of PET is its low ability to maintain its general shape in molten status.

Nylons, or polyamides (PA) is formed by condensation polymerization of a diamine and a dibasic acid or by polymerization of certain amino acids.

Polyamides in general provides good optical clarity, resistance to oil and chemicals and also has high mechanical strength over wide range of temperatures. In packaging the use of PA is mostly found in the form of films used for high temperature sterilization. PAs also act as flavour and gas barriers but have poor water vapour barrier properties.

Paper and paper board are also one of the mostly used materials for packaging in the world. Paper can be obtained from plants fibers. More than 95% of paper is obtained from wood and very small amounts are mainly agricultural by-products such as straw (of wheat, barley and rice), sugar cane bagasse, cotton, flax, corn husks, and so on. Different varieties of papers are used in packaging applications.

Metals are used for packaging a variety of products. These products include tuna cans, can drinks etc. For food packaging, four types of metals are mostly used. These include; steel, aluminium, tin and chromium. Steel and aluminium are commonly used in production of food cans of different varieties like beverage cans and tuna cans. Steel tends to oxidise when exposed to moisture and oxygen. This is termed as rusting. Therefore, tin and chromium are used as protective layers for steel.

Glass has a very good and lengthy history in food packaging [64]. In food packaging applications, bottles or jars are the types of glass that is mostly used with bottles being used commonly. In the US, 75% of all glass food containers are bottles. Glass has its primary constituents to be silica, which is derived from the sand or sandstone. For most glass, silica is combined with other raw materials in various proportions. For example, the glass typically

used for food packaging, soda-lime glass contains silica (68-73%), limestone (10-13%), soda ash (12-15%), and alumina (1.5-2%). Glass is mostly inert to a wide variety of food and non-food products. It is very rigid, transparent and non-permeable (excellent barrier properties). However, glass is heavy, sharp and very brittle hence limits its use in food packaging. The fragility of glass has caused some safety concerns such as the possibility of the presence of chipped glass in food products. This has declined the use of glass as food packages over the last three decades and has diminished in marketability as compared to metals and plastics. Though it still plays an important role in packaging [13].

2.6 Mechanical modelling and simulations of composites

The mechanical properties of a composite materials can be modelled with abaqus CAE software. Abaqus is a software suitable for finite element analysis and computer-aided engineering. The first release date for this software was in 1978. It has applications in automotive, aerospace and industrial products industries.

In these industries, users can define their own material models so that the sample could be modelled. Abaqus can also be used to provide multiphysics capabilities such as coupled acoustic-structural, piezoelectric and structure-pore.

The steps involved in using abaqus software for modelling are pre-processing, evaluation and simulation, post-processing (Visualization).

The pre-processing involves creating an input file which contains an engineer's design for finite-element analyser. In the design, the material is specified, boundary conditions, load, and

mesh is also assigned to the design. The second step is to produce an output file by analysing the job. After analysing the job, the report is generated from the visualization stage [70].

CHAPTER THREE

3.0. MATERIALS AND METHODS

This chapter focuses on the experimental methodology that were used in the work. The materials, equipment and chemicals that were used as well as the sample preparation method and characterization methods that were used is discussed in this chapter.

3.1 Sources of materials and equipment used

Cassava starch was extracted from cassava tubers purchased from Madina market in Accra, Ghana. Nanokaolin, a particulate modifier was obtained from Teleku Bokazo a town with deposits of this raw material in the Ellembele district of the Western Region, Ghana. Glycerol and distilled water was obtained from Timstar laboratory suppliers ltd. Glycerol (Propane 1,2,3-triol) had purity of 99 %, molecular weight of 92.10 and refractive index of 1.471 to 1.473. Cellulose nanofiber was extracted from rice husk obtained from Abaam in the Eastern Region.

The equipment used during the preparation of thermoplastic starch (TPS) are; heating plate, electronic balance, measuring cylinder, beaker and stirrer.

3.2 Material Preparation

3.2.1 Starch Extraction

The cassava was soaked in a clean bowl containing water for 24 hours before it was peeled. The peeled tubers were then cut into smaller pieces capable to be blended. After blending, 10 litters of water were added to the 860g of blended cassava and stirred rigorously. The mixture obtained was sieved with a cotton cloth. The resulting filtrate was left undisturbed for another 24 hours to allow the starch to settle at the bottom of the bowl. Another 10liters of water was added to the solid residue from the sieved cassava blend. The resultant mixture was sieved

again and the filtrate left undisturbed for 24 hours. After 24 hours in both bowls, the mixture was decanted leaving only the starch at the bottom of the bowl. The starch was sun dried for 3 days and processed into fine particles by dry blending to give 300g of starch.

To test for the fitness of the cassava starch extracted, two drops of 0.01M iodine solution was added to solution of starch and water and the colour change was observed. The colour changed to blue-black which confirmed the product extracted to be starch.

3.2.2 Clay milling

To achieve fine particle of the clay, it is required that, the clay is continuously milled for longer periods of time. The particle size required for this work is in the range 120μm-100nm.

This is due to the application for which the clay were employed. These particle sizes are required in packaging applications because in these size scales, the pore sizes are very minute to allow much matter (water vapour and gas) into and out of the enclosed space. This will aid the packaging material to serve the purpose of maintaining the integrity of the product, and protect the product from environmental attack.

The mill that was used to achieve the required particle size range in this research was the PQ-N4 planetary ball mill. The milling medium was alumina balls and the frequency for milling was adjusted to 35 Hz to mill the sample for 5 hours. Equal amounts of the nanokaolin were measured into the four bowls and fixed into the equipment. The equipment was then powered on and the samples allowed to mill. After milling, the clay particles were sieved to obtain the required size using a 120μm pore sieve.

3.2.3 Extraction of cellulose nanofibers from rice husk

Rice husk was obtained from a local rice producing company in Abaam located in the Kwaebibirem district of the Eastern Region. Rice husk was grinded into fine particle and sieved

with a 120 micrometre sieve. After sieving, the powder material was treated with an alkali and acid. From similar work done by Hunani et al. and Yeng in the extraction of cellulose from rice husk, the chemicals that were used include Sodium hydroxide (NaOH), Nitric acid (HNO_3) and Sulphuric acid (H_2SO_4) [7], [31].

Rice husk was treated 1.0 M Nitric acid at room temperature under mechanical stirring for 24 hours and washed with distilled water until the pH was 5.0 [62], [26].

Sodium hydroxide (1 M, NaOH) was added to the rice husk treated with nitric acid and stirred at room temperature for another 24 hours. After 24 hours, the solution was filtered using the suction filtration and the residue was wash severally with distilled water which helped to remove the residual additives such as partially solubilised pectin, lignin, and hemicellulose impurities. The washed residue was reacted with 6 M Sodium hydroxide solution whiles stirring at room temperature for another 24 hours. Sulphuric acid (4 M) was added to the residue after 24 hours of reacting with 6 M Sodium hydroxide under constant stirring. This solution was stirred for 6 hours and then filtered using the suction filtration method. The residue was washed severally with distilled water until the pH was in the range of 5-6 [31]. The final product was then kept in a plastic container. Figure 3.1 is a summary of the method for extracting cellulose from rice husk.

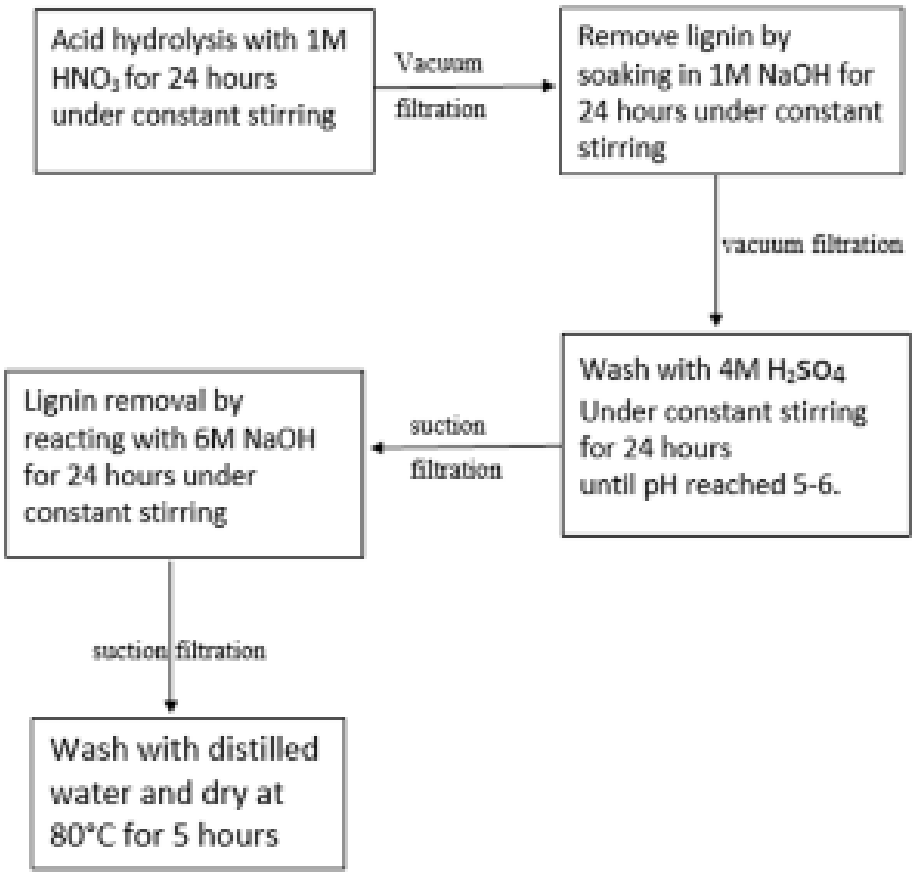

Figure 3.1 Flow chart of cellulose nanofiber extraction from rice husk

3.3 Biocomposite batch formulation and fabrication

The fabrication of the biocomposite begun with batch formulation of the samples and followed by the stepwise fabrication.

3.3.1 Batch formulation

The biocomposite were prepared with respective amounts of starch, glycerol, water, nanokaolin, cellulose nanofiber. The mass of starch, volume of glycerol and water were kept constant throughout the starch biocomposite sample preparation. The content of nanokaolin, cellulose nanofibers was varied in volume fractions from 0.1 – 0.4.

Table 3.1a and b shows the batch formulations of the various biocomposites and their contents that were prepared. For each formulation, 45ml of distilled water and 3ml of glycerol was added to make the biocomposite plastic. The designations and naming of the samples are shown in table 3.1a and b.

Table 3.1a Batch formulation for TPS-nanokaolin biocomposites.

Sample	**Starch (grams)**	**Clay (grams)**
TPS only	10	0
TPS-0.1 Kaolin	10	1.0
TPS-0.2 Kaolin	10	1.9
TPS-0.3 Kaolin	10	2.9
TPS-0.4 Kaolin	10	3.9
TPS-0.5 Kaolin	10	4.9

Table 3.1b Batch formulation for TPS-cellulose biocomposites.

Sample	**Starch (g)**	**Cellulose nanofibers (g)**
TPS only	10	0
TPS-0.1 Cellulose	10	1.0
TPS-0.2 Cellulose	10	1.9
TPS-0.3 Cellulose	10	2.9
TPS-0.4 Cellulose	10	3.9
TPS-0.5 Cellulose	10	4.9

3.3.2 Preparation of starch biocomposites by solution casting

Biocomposite composed of starch, nanokaolin and cellulose nanofiber were prepared by mixing various quantities of materials required in every batch using the batch formulations above. Glycerol content used in preparing the biocomposite was 3ml and the amount of water used was 45ml. For the various biocomposites, the amount of starch needed as shown in table 3.1a and 3.1b was measured into a beaker using an electronic balance and the glycerol and water was added to the starch in the beaker and stirred continuously. The mixture is then heated and stirred continuously at 125 °C and 60 rpm respectively until a gel is formed. The gel was then poured out into the required moulds and some onto a flat glass surface and pressed into thin films. The prepared sample was then sun dried for 5 days and removed for testing.

Batches that contain modifiers are prepared in the similar way as samples without modifiers. For starch-clay composites, the clay is added to the solution of starch, glycerol, water and stirred to achieve homogeneity before heating to form the composites.

For starch-cellulose composites, the gel formed after stirring the mixture of starch, water, glycerol under constant temperature is added to the cellulose crystals and stirred thoroughly before pouring into the moulds to form the biocomposites.

3.4 Modelling of Mechanical Properties with Finite Element Analysis software

The models designed for this research was derived from the analytical aspect taken from the basic rule of mixtures for composite materials. The steps required to analyse and simulate a model includes define the geometry, assign the material property, assign the boundary conditions, assign the load, mesh the geometry into squares, triangles, hexagons etc.) and finally analysing the Von misses stress distributions. After designing, or sketching the part, the rule of mixtures theory is applied to assign the material property.

3.4.1 Geometry Definition

The geometry that were modelled for the simulations were the bone-shape model for tensile test. Figure 3.2 shows the geometry for tensile test and bending test respectively. The dimensions used in sketching the model part are shown in table 3.2.

Table 3.2 Part dimension for tensile (bone-shape) model

Part description	**Dimension(mm)**
Width of reduced section	11
Thickness	3
Radius of fillet	4
Overall length	80
Grip Length	6
Length of reduced section	63
Width of grip section	21

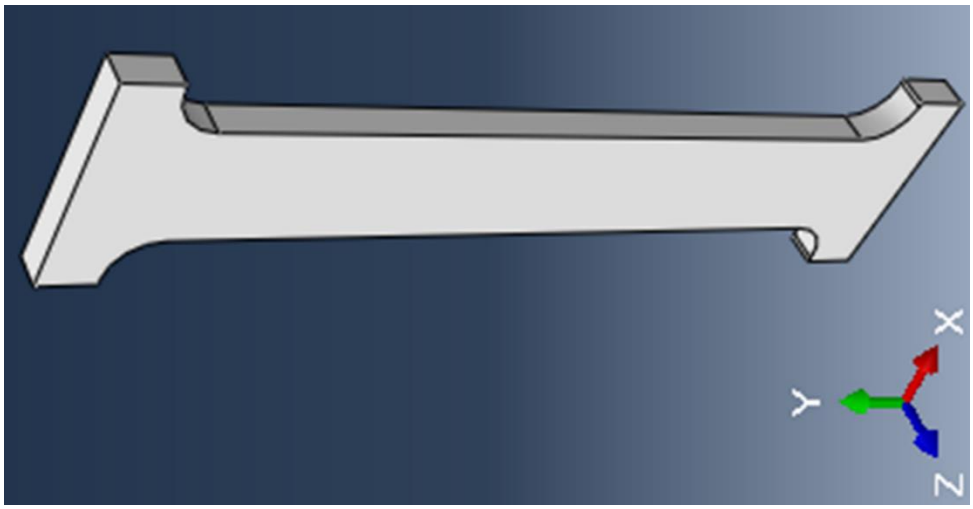

Figure 3.2 Bone shape geometry for tensile test

3.4.2 Assign material property

The materials that were assisnged in the numerical modling of the biocomposite are starch, nanokaolin and the fiber. The required material properties that are required are the Young's modulus of elasticity (E) and the poisson ratio (ϑ). Again from the analytical modelling with the application of the rule of mixtures theroy, the elastic modulus of the composite was calculated using the individual material modulus of elasticity. The poison ratio used for the modelling is also stated in table 3.2. The individual elastic modulus of the materials used is also shown in table 3.2.

Table 3.3 Materials and their mechanical properties used for modelling

Material	**E (GPa)**	**Poisson ratio**
Starch	2.7	0.4
Nanokaolin	13	0.36
Cellulose Fiber	12	0.30

Using the volume fraction stated in table 3.3 [25], [74], [47], [57], [56], the elastic modulus of the composite that was used in modelling various biocomposites is shown in table 3.4.

Table 3.4 Elastic modulus, poisson ration of composites used in modelling

Model	**Volume fractions starch**	**Elastic modulus of biocomposite (GPa)**	**Poisson ratio of biocomposites**
TPS only	1.0	2.7	0.4
TPS-nanokaolin	0.9 0.8 0.7 0.6 0.5	3.73 4.76 5.79 6.82 7.85	0.38
TPS-cellulose	0.9 0.8 0.7 0.6 0.5	3.63 4.56 5.49 6.42 7.35	0.34

3.4.3 Assign boundary condition and load

The step named initial was held fixed and used as the boundary condition. The cordinate systems of the boundary condition was held constant. After asigning the boundary condition at the initial step, the load was created.

To create the load, a new step was created and the increment from the initial step was 0.1. The load was created at the pull load step. The magnitude of the load that was used in simulating was 30 N in tension. Figure 3.3 shows the pictorial view of the boundary condition and load assigned to a dog-bone shape tensile test model.

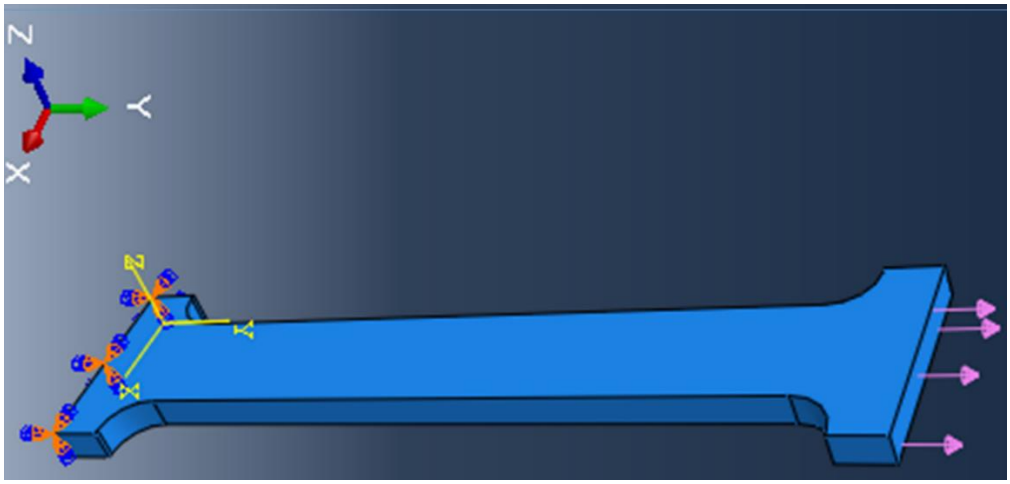

Figure 3.3 model showing the boundary condition and load

3.4.5 Mesh geometry

The part is meshed into hexagonal shapes from the assign mesh control module. In this section, a global seed is assigned and the element type and mesh controls are all assigned. After going through the various processes, the part is meshed successfully and the model is ready to be analysed. After following the steps, the model is seen to be divided into smaller portions as shown in figure 3.4.

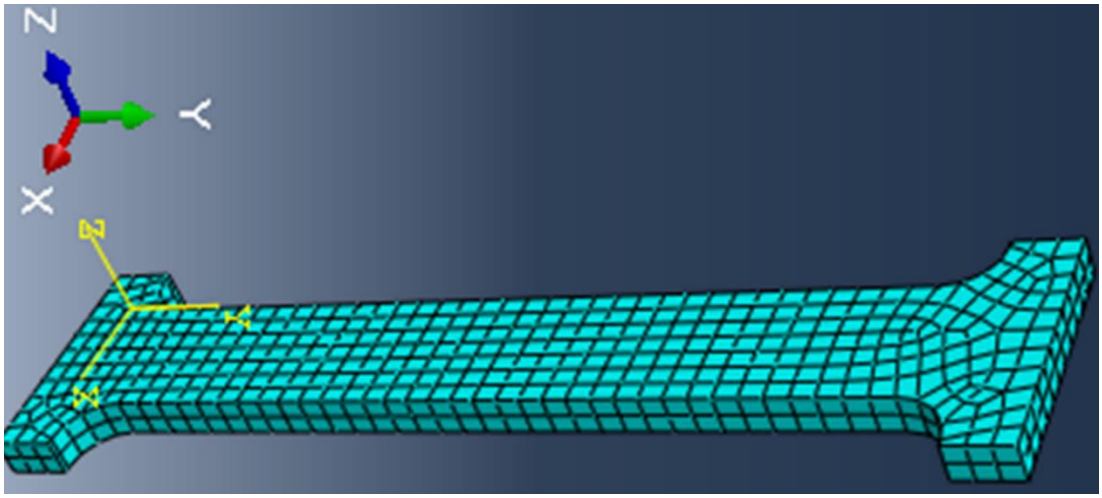

Figure 3.4 meshed model

3.4.6 Analysis of Von Mises stress distributions

In the real world; practically, there is not any much time for one dislocation to start and complete before another dislocation starts. Hence this becomes difficult if one wants to analyse the stresses. However, Tresca criterion can be applied in real life to calculate stresses.

In order to account for the step by step dislocation of slips in a material, we can apply the Von-Mises criterion. In this analysis, the start and finish of a dislocation is accounted for before another begins.

In this model, the von mises streses is analysed to know which stage or points on the sample that experienced high streses. This can be seen because the Von-Mises stress is analysed for every part of the model and this is done step by step.

3.5 Characterization

The samples were characterized to know their mechanical, physical and chemical properties. The techniques employed include Fourier Transform Infrared (FTIR) Spectroscopy, Scanning Electron Microscopy (SEM), tensile test, water vapor permeability test and X-ray Difractomery (XRD).

3.5.1 Fourier Transform Infrared (FTIR) Spectroscopy

FTIR Spectroscopy is an analytical technique used to identify organic, polymeric, and, in some cases, inorganic materials. The FTIR analysis method uses infrared light to scan test samples and observe chemical properties. FTIR analysis can be used to identify and characterize unknown materials (e.g., films, solids, powders, or liquids), identify contamination on or in a material (e.g., particles, fibers, powders, or liquids), identify additives after extraction from a polymer matrix, identify oxidation, decomposition, or uncured monomers in failure analysis investigations [60].

The FTIR equipment used was the Bruker-Alpha Platinum-ATR machine. This characterization technique gives ideas about the structural orientation of the biocomposite. This can be achieved by determining what compounds or chemicals are present in the biocomposite. The samples used for this characterisation were prepared by being cleaned thoroughly with ethanol to prevent contamination and also to do away with any unwanted printing on the surface. Similar to the sample preparation, background checks are run on the equipment and cleaned thoroughly before mounting the sample on the stage for characterization. This characterization technique was considered for control sample and the TPS-nanokaolin sample, without taking into consideration the volume fraction of the nanokaolin component. The volume fraction of the clay component was not considered because it was assumed that chemical component of the sample were the same despite changes in composition. The same was done for TPS-cellulose samples.

In principle, infrared spectroscopy probes the sample for molecular vibrations with an infrared source which when absorbed, can be associated with characteristic infrared absorption bands [44], [54].

3.5.2 Scanning Electron Microscopy (SEM)

A scanning electron microscope scans a focused electron beam over a surface to create an image. The electrons in the beam interact with the sample, producing various signals that can be used to obtain information about the surface topography and composition.

The SEM equipment used in this characterisation is the Phenom ProX SEM desktop machine. It is located at the Earth-science department at University of Ghana. The equipment was operated in backscattered mode with the 15Kv source of electrons bombarded unto the specimen. The most important step to observing the morphology is sample preparation. During

sample preparation, the test specimen which is non-conductive is made conductive by coating with platinum (Pt) at 30 mA and 15kV. This was done at the Animal biology SEM laboratory. This was to make the sample conducted to the bombarded electrons.

SEM technique does not affect the chemical nature of clay samples. It is a very informative technique to identify the structure and chemical composition of any material including raw clay, pure clay materials and its derivatives.

3.5.3 Energy Dispersive X-ray spectroscopy (EDX)

The characterisation is normally performed in conjunction with the scanning electron microscopy technique. It is an analytical technique used for elemental analysis or chemical characterisation of a samples. It is done to analyse the elements and their respective quantities in the sample being studied. The principle from which this analytical technique operates is similar to that of XRD analysis technique. It relies on an interaction of some source of X-ray excitation unto a sample which contains unique atomic structure allowing unique set of peaks on its X-ray spectrum.

3.5.4 X-Ray Diffraction Analysis (XRD)

After preparing the biocomposites also, they were taken for XRD analysis. Here, the analysis was conducted with the Bruker XE-T 2nd generation D2 Phaser XRD machine which is equipped with CuK anode radiation source operated at a generator tension of 30 kV and a generator current of 10mA. Samples which were thin films were scanned from 5° to 65° within 20 minutes.

3.5.5 Tensile Test

Tensile testing is a fundamental materials science and engineering test in which a sample is subjected to a controlled load in tension until failure. Properties that are directly measured via

a tensile test are the loads applied to the specimen and percent elongation of the specimen. The data obtained from the tensile testing (load, time) was used to obtain a stress-strain diagram from which the fracture strength, yield strength and ultimate tensile strength were determined. However, tensile tests were conducted on all the samples to determine the percentage elongation and also obtain the stress-strain diagram for all samples.

For this characterization technique, four samples were tested per each composition of various nanokaolin constituents. However, for TPS-cellulose biocomposites, two samples each were taken for the tensile test. The samples were labelled taking into consideration the volume fraction of nanokaolin and cellulose nanofiber present. The geometry of the sample was such that they took the design and shape of a bone. For the bone shape specimen, the dimensions that are of importance to aid the determination of the tensile strength, tensile strain, tensile modulus of elasticity are the thickness, width, gauge length and final length. Figure 3.5 shows the mould that was used in casting the (tensile-bone shape) biocomposites.

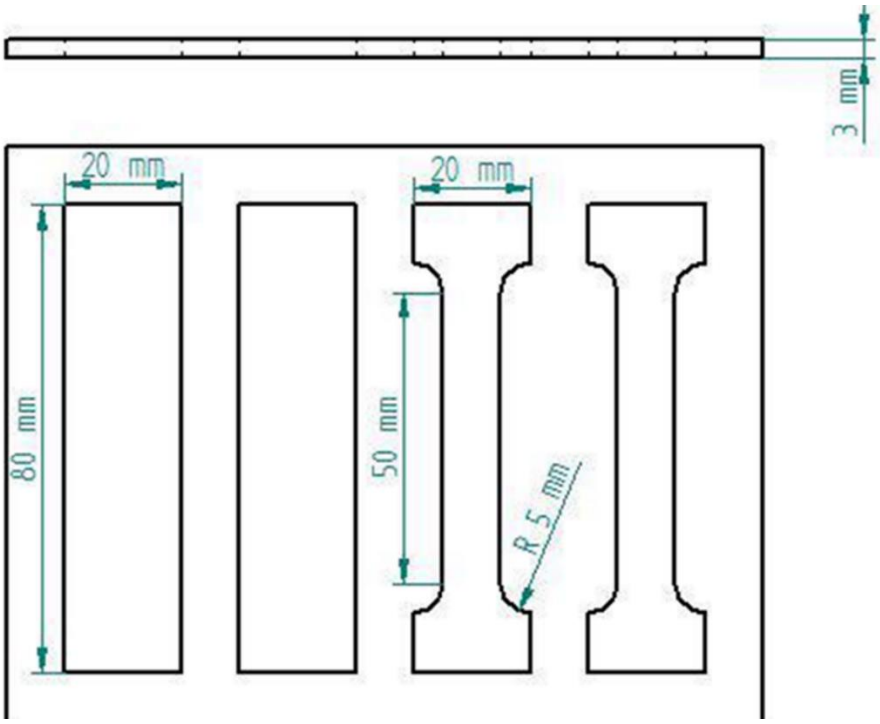

Figure 3.5 Tensile test (bone-shape) mould dimension for biocomposites

The mechanical tensile test machine was operated with a speed of 20mm/min. After adjusting the speed, the samples to be tested were fixed in the grip of the machine and the loading started. Before fixing the specimen to be tested into the grip, the thickness, width and gauge length were measured. The loading of the machine was started simultaneously with a computer which was used to record the data by the help of the mechanical tensile test software. After the specimen had deformed, the final length, width and thickness of the specimen was also measured. The data recorded shows the load as the specimen was deformed and the various times of deformation. This data was used to calculate the strain rate, stress, and the strain of the specimen tested was also determined from the measured initial and final length.

Another important deduction the stress-strain curve is to tell which material is more plastic and which one is more elastic. Figure 3.6 shows a similar stress-strain curve and the different designations on them.

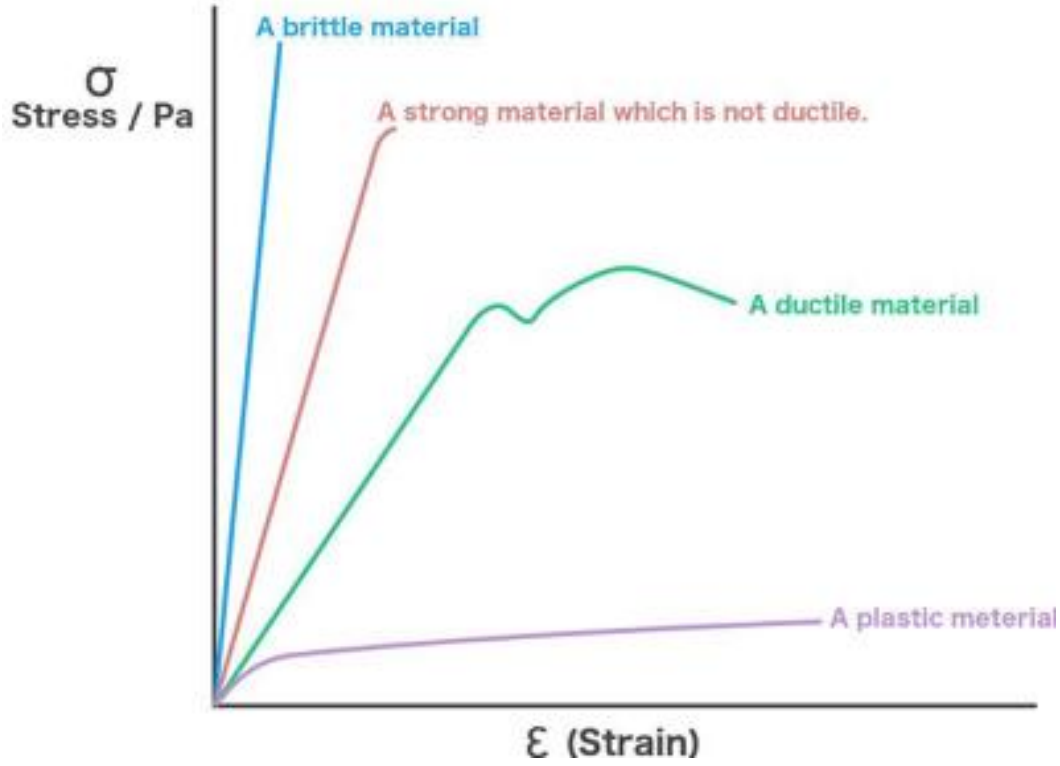

Figure 3.6 Stress-strain curve for different materials [5].

The diagram in figure 3.6 shows the response of four different materials to tensile loading. The four materials are brittle materials, strong but not ductile materials, ductile materials and plastic materials.

A brittle material deforms elastically and have a high young's modulus. This type of material is able to resist some amount of deformation but very sensitive to shock and breaks easily.

A strong material that is not ductile, is highly elastic but less plastic. Plastic materials are also known to have small elastic and large plastic region. These materials are easy to deform and nearly insensitive to flaws and shocks.

Strong and tough also known to be ductile combine high Young's modulus with a plastic deformation. These materials resist well to deformation and shocks as well as being insensitive to flaws and deflects.

3.5.6 Water vapour permeability test

One important function of packages is to maintain the moisture content of a product. The package either helps to keep the product dry or moist. This test method covered the determination of water vapour through the specimen. This is done to determine the ability of the packaging film to resist moisture transmission. According to ASTM E96, this characterization technique can be applied to specimen of thickness not over 32mm [9].

The sample to be used for this test was prepared into a thickness of 0.4mm. The samples were prepared for control as well as cellulose nanofibers and nanokaolin volume fractions of 0.1, 0.2, 0.3, 0.4 and 0.5.

After preparing the samples, it was dried in the sun for 3 days before testing for the water vapour transmission.

The standard used in this research is ASTM E96/E96-05, where the desiccant method is used to test for the water vapour permeability test. In this test, the desiccator is filled with the desiccant about 10mm below the wire plate. After placing the desiccant in the desiccator, the sample is placed on a beaker filled with 10 ml of water and tightly sealed. The beaker containing water and the sample covering it is weighed and then placed in the desiccator. The desiccator is then placed in a controlled environment for one day (24 hours).

3.5.7 Thermal Properties

The thermal properties were characterized using TGA and DSC analysis technique. In TGA, the mass of the sample being analysed is observed as the temperature is changed to determine the rate of mass loss of the sample with temperature. The device used for the TGA analysis was the NETZSCH TG 209F1 device and nitrogen gas (N_2) was the atmosphere where the samples were scanned.

In DSC, the heat flow of the sample was measured against the change in temperature at particular time intervals. Thermograms were generated after this analysis technique. The themogram gives the deviation of the heat signatures of the sample from the reference material. Any deviation above the reference heat line is known to be exothermic whiles any deviation below the reference heat line is known to be endothermic. The area under the curve peak also gives the amount of heat energy that is absorbed or released. The atmosphere where DSC is conducted is nitrogen gas (N_2).

CHAPTER FOUR

4.0. RESULTS AND DISCUSSION

4.1 Microstructural Characterisation

These test were conducted to show the chemical compositions of the sample and also to show the morphology and crystallinity of the sample.

4.1.1 Fourier Transform Infrared Spectroscopy (FTIR)

The FTIR spectra of the biocomposites, as presented in Fig. 4.1, 4.2 and 4.3. FTIR was able to identify the interaction between polymer functional groups as well as the characteristic bonding of OH. In principle, the infrared that is released from the source, can be absorbed by the sample which causes molecular vibration that makes the molecules on the sample being characterised to stretch, stress, compress and bend.

The FTIR results is reported with a graph of transmittance against the wavenumber.

From the graph of transmittance against the wavelength of the infrared source, figure 4.1 shows the IR spectra for TPS only which contains no nanokaolin or cellulose nanofibers whiles figure 4.2 and 4.3 corresponds to the IR spectrum of the TPS-nanokaolin and TPS-cellulose biocomposites respectively.

The bands of the ftir results were similar to that of bands for glycerol which was obtained from literature [39].

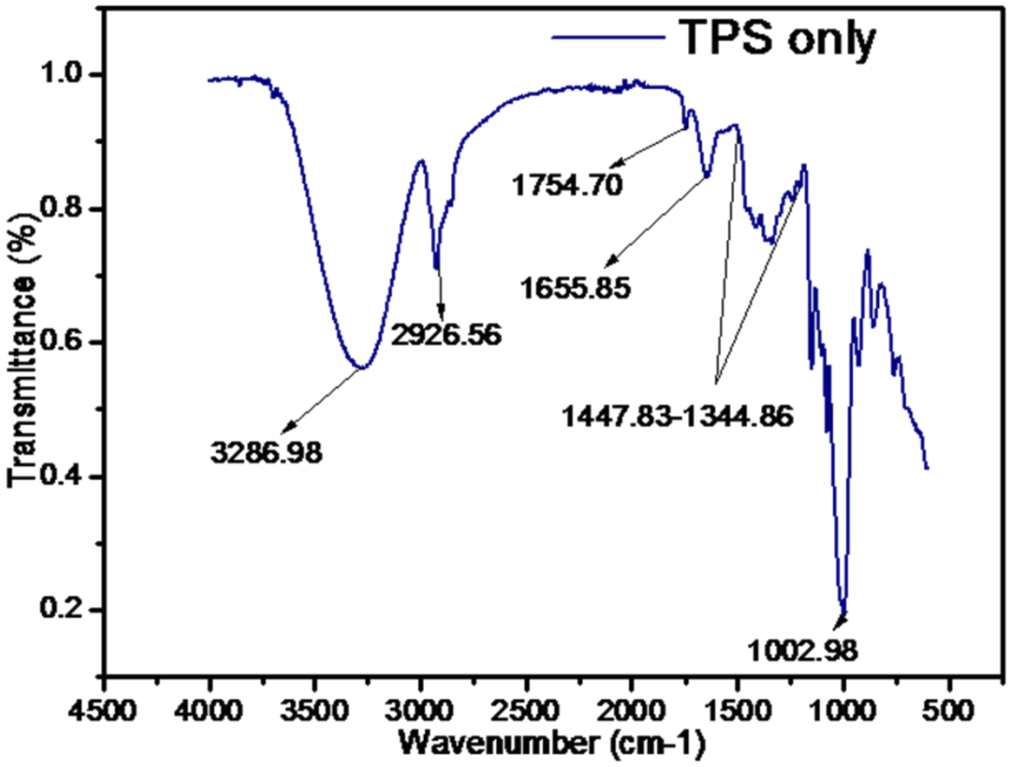

Figure 4.1 FTIR bands and peaks for TPS only

The main bands of the control specimen are at 3286.98 cm^{-1}, 2926.56 - 2852.65 cm^{-1}, 1655.85 cm^{-1}, 1447.83 – 1344.86 cm^{-1} and 1002.98 cm^{-1}. The bands responsible for the OH stretching modes of water and glycerol is usually reported at band ranges of 3000 – 3600 cm^{-1} [23]. However, for this research, the stretching vibrations of OH groups present in the chemistry of starch and glycerol was recorded at 3286.98 cm^{-1}, whereas the band at 1655.85 cm^{-1} is mainly due to OH bending mode of water molecules that was used as solvent in mixing the starch.

The other peaks of the control specimen are mainly due to the reaction of starch with glycerol. The peaks around 2926.56 – 2852.65 cm^{-1} are due to the CH stretching modes of starch-glycerol reaction whereas the peaks between 1447.83 – 1344.86 cm^{-1} is reported as the in plane CH_2 bending of molecules in starch. The band at 1002.98 cm^{-1} is reported as C–O stretching modes in C-O-H and C-O-C in glucose ring [73].

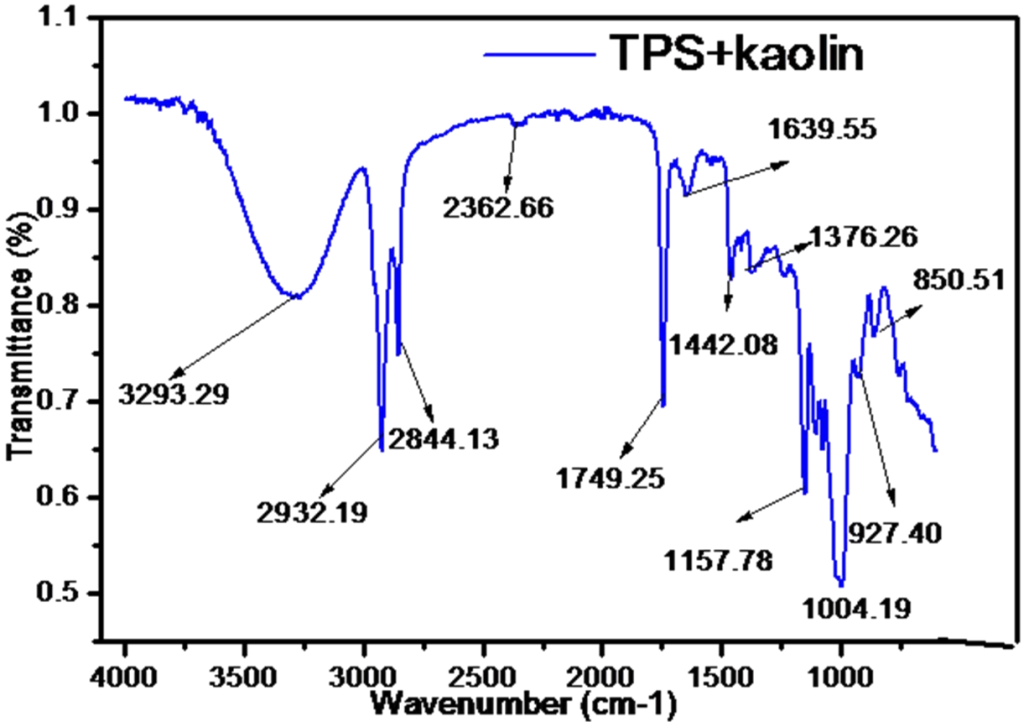

Figure 4.2 FTIR bands and peaks for TPS-nanokaolin composites

The main bands of the TPS-nanokaolin specimen are at 3293.29 cm^{-1}, 2932.19-2844.13 cm^{-1}, 2362.66 cm^{-1}, 1749.25-1639.55 cm^{-1}, 1442.08-1376.26 cm^{-1}, 1157.78-1004.19 cm^{-1}, 927.40-850.61 cm^{-1}.

The bands peaks are similar to that shown in the IR peaks or bands for the control specimen with the bands at 3293.29 cm−1 representing OH stretching, 2932.19-2844.13 cm^{-1} representing CH stretching modes of CH_2 present in starch and glycerol groups with the increase of intensity of the band at 2932.19 cm^{-1} [46].

The peak at 2362.66 cm^{-1} is reported to be amide which can be as a result of the introduction of nitrogenous compounds in starch matrix during fabrication. The band at 1749cm^{-1} and 1639.55 is reported to be in plane bending of CH and OH bending mode of water molecules respectively, as reported in the control sample. C–O stretching normally of glucose ring was also reported at band 1004.19-850.61 cm^{-1}.

The peak at 1157.78 cm^{-1} indicated that of the Si–O–C bond which is reported in literature to be associated with an H-bonded Si–OH group. This is normally produced from the reaction between starch and silicate phase of clay [46].

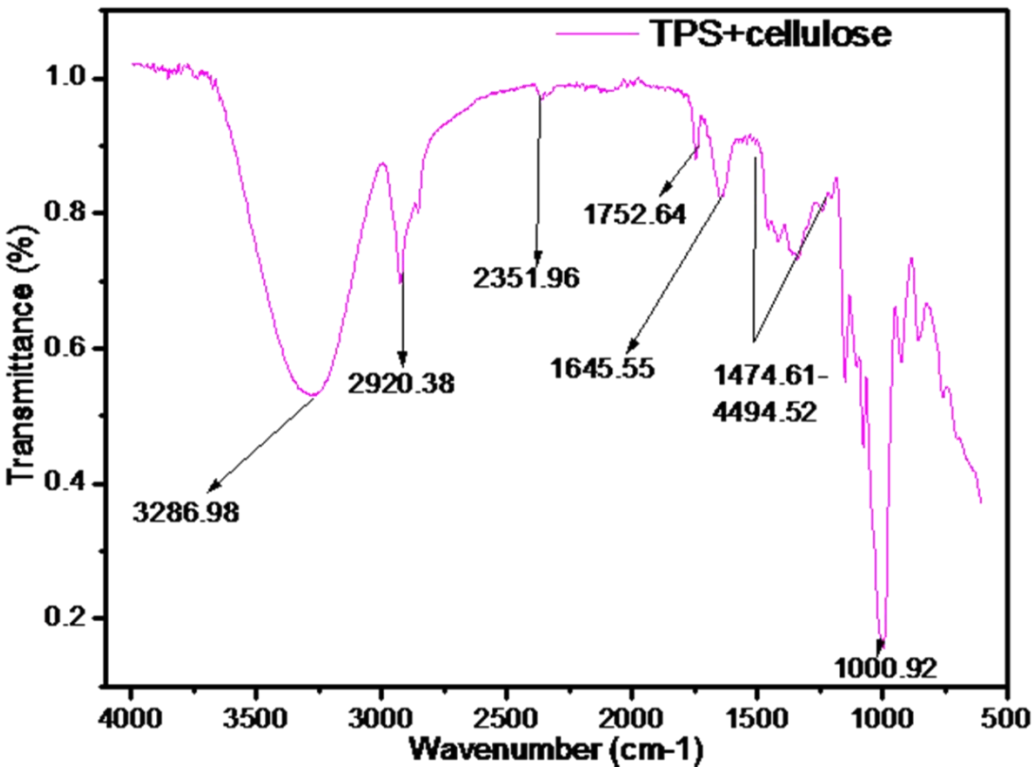

Figure 4.3 FTIR bands and peaks for TPS-cellulose composites

The main bands of the TPS-cellulose sample are reported to be 3286.98 cm^{-1}, 2920.38 cm^{-1}, 2351.96 cm^{-1}, 1752.64-1645.55 cm^{-1}, 1474.61-1194.52 cm^{-1} and 1000.92 cm^{-1}. Some of these bands are similar to the bands that were recorded for TPS and TPS-nanokaolin samples respectively.

The band for OH stretching which is of the polysaccharide group was recorded at wavenumber of 3286.98 cm^{-1}. This band indicates H-bonding interactions in these materials.

The peaks observed at 2920.38 cm^{-1} correspond to –C-H stretching [48]. The band at 2351.96 cm^{-1} is reported to be amide which can be as a result of the introduction of nitrogenous compounds in starch matrix during fabrication. This band was reported in TPS-nanokaolin at

wavenumber of 2362.66 cm^{-1}. However, in TPS sample, this band was not observed clearly. Bands for OH bending of water molecules were observed at 1752.64-1645.55 cm^{-1}. The peaks between 1474.61-1194.52 cm^{-1} is reported is similar to the peak recorded for TPS sample in figure 4.1 at wave number of 1447.83 – 1344.86 cm^{-1}. This band is recorded as the in plane CH bending of CH_2 molecules in starch.

The band for C–O stretching modes in C-O-H and C-O-C in glucose ring is recorded at wavenumber of 1000.92 cm^{-1} for TPS-cellulose biocomposite [73].

4.1.2 Scanning Electron Microscopy

Images generated from the analysis is reported in this section. The samples that are reported in this section are the cellulose nanofiber, TPS-nanokaolin biocomposites and TPS-cellulose biocomposites. The images taken showed the distribution of the particles and fibers in the matrix face of the biocomposite.

4.1.2.1 SEM image of Cellulose nanofiber

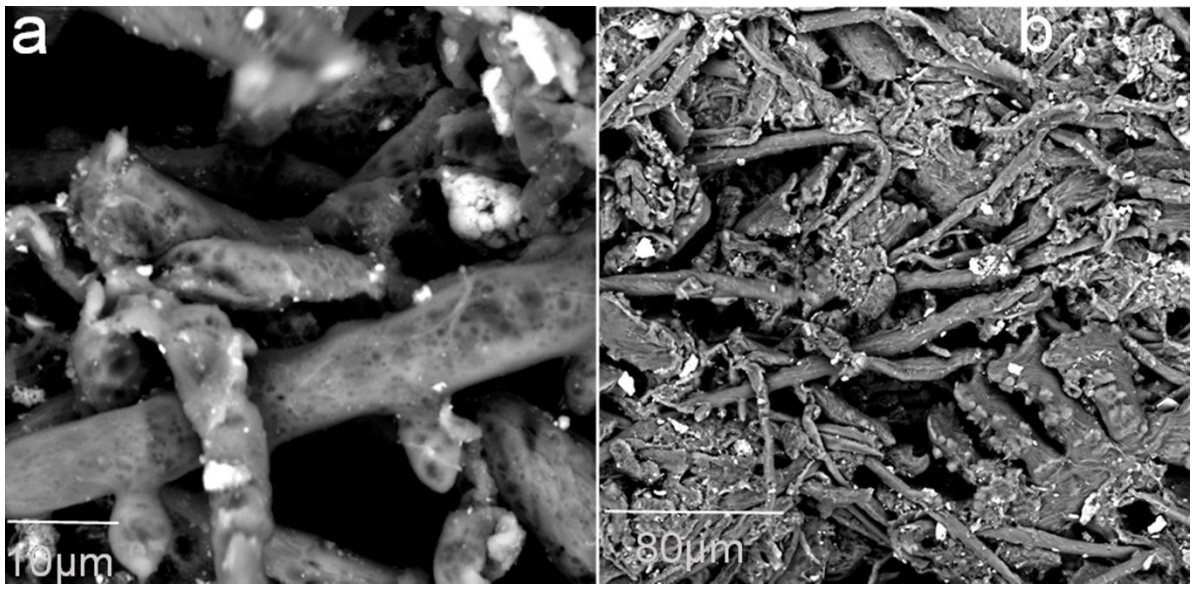

Figure 4.4 SEM image of the microstructure of cellulose nanofiber

Figure 4.4 is the microstructural images of cellulose nanofibers at 5000X and 1000X magnifications. The image at 1000X (a) magnification shows the weblike nature of the cellulose nanofibers. The cellulose nanofibers are seen to be intertwined with itself in the microstructural image shown in figure 4.4(a) at 5000X magnification.

4.1.2.2 **SEM image of thermoplastic starch (TPS)**

The micrographs of TPS only films are shown in Figure 4.5. The surface morphology of the film as in figure 4.5a showed a relatively smooth and continuous layer by layer morphology which confirmed a dense and homogeneous structure taken at a magnification of 1600X. However, at a magnification of 6200X and 3200X, as shown in figure 4.5b and 4.5c respectively, it is noticed that there is a patchy and rough cross-section which may be associated with the flexibility of starch polymer in the network of starch-glycerol films.

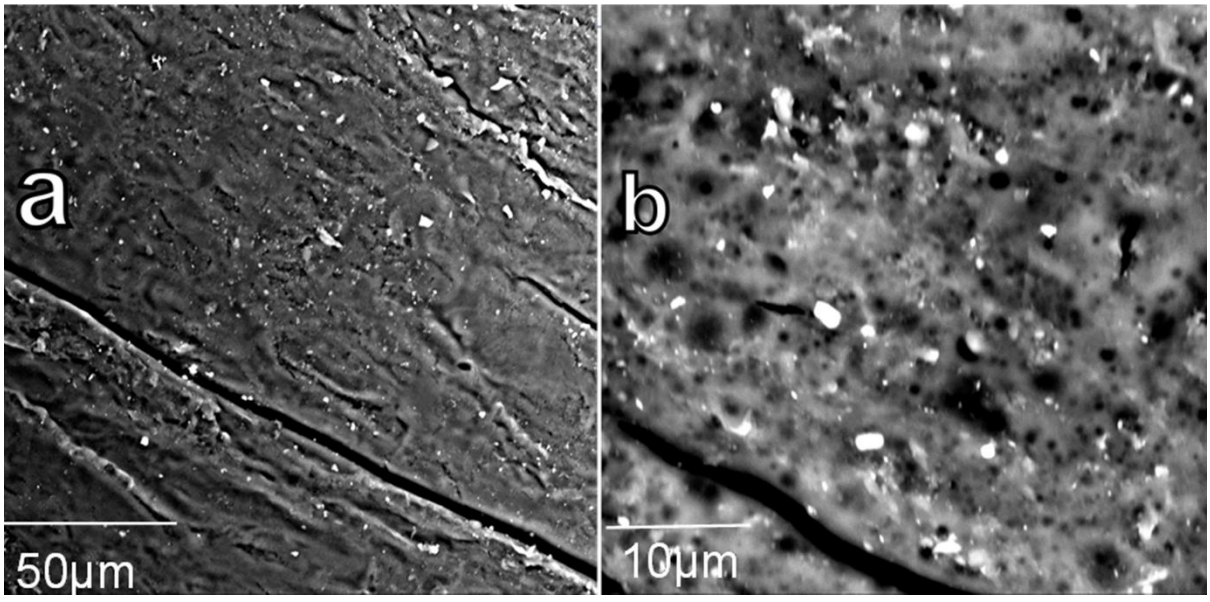

Figure 4.5 (a), (b) SEM images of TPS only

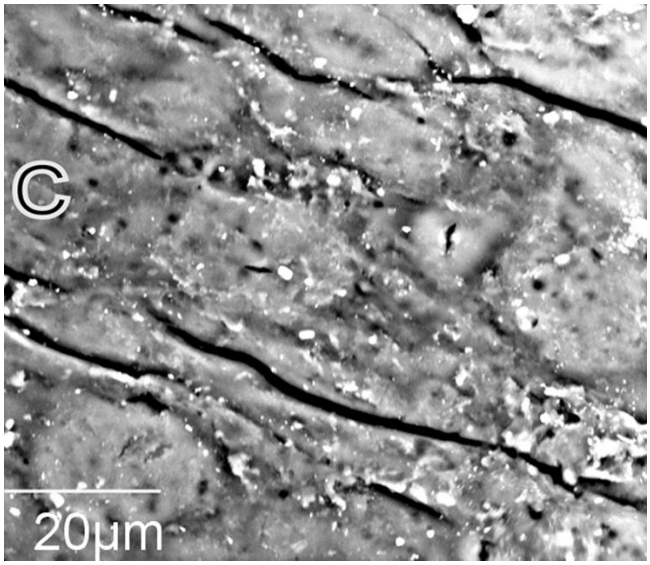

Figure 4.5 (c) SEM images of TPS

4.1.2.3 SEM image of TPS-nanokaolin Biocomposites

Images for TPS-nanokaolin biocomposites were taken at magnifications around 1500X, 3000X and 6000X. The images were taken to confirm the presence of nanokaolin in the biocomposite and also to show the distribution and arrangement of the clay (nanokaolin) particles in the TPS matrix. Figure 4.6 a,b,c and d shows the images of the TPS-nanokaolin biocomposites.

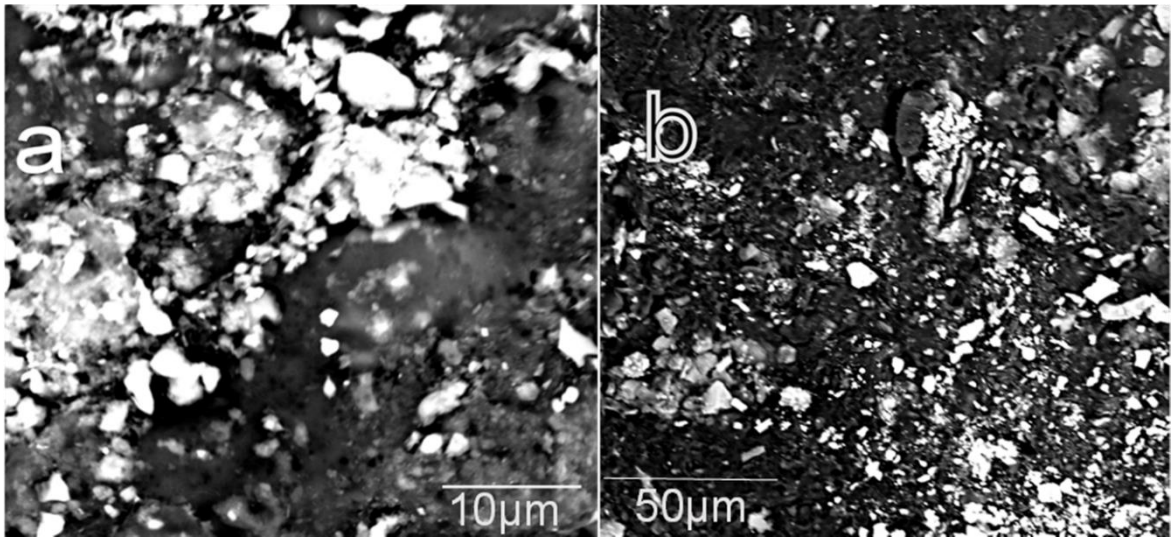

Figure 4.6 (a) and (b): SEM images for TPS-nanokaolin

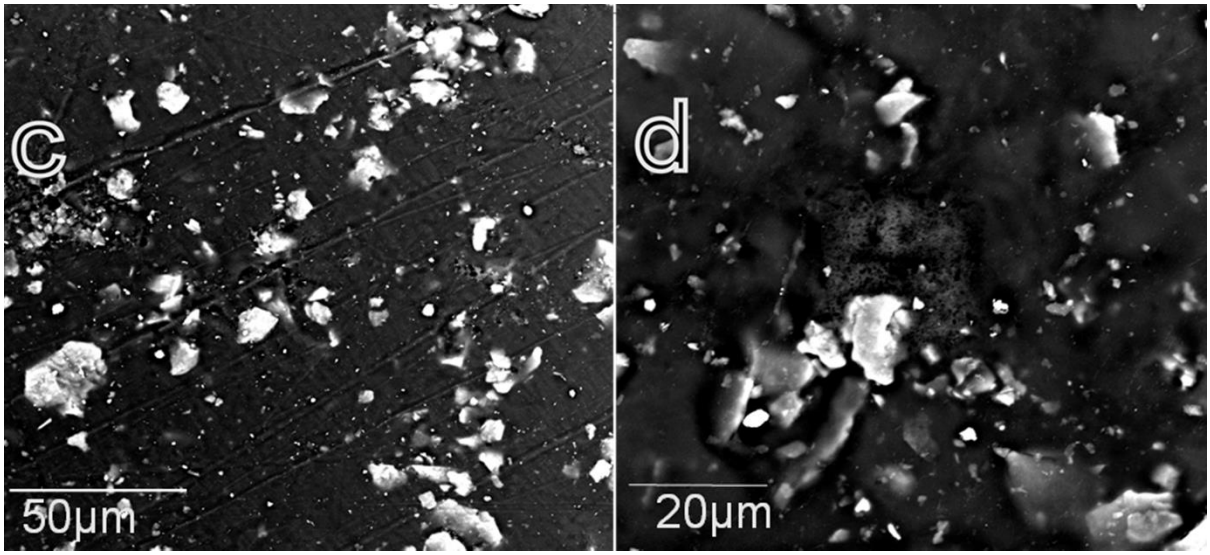

Figure 4.6 (c) and (d): SEM images for TPS-nanokaolin

The images shown in figure 4.6 a, b, c and d, shows dark phase of TPS matrix and white phases of nanokaolin distributed in TPS matrix. From the microstructural images, it is noticed that the nanokaolin phases are uniformly distributed in some portions of the biocomposite and non-uniformly distributed in other portions.

4.1.2.4 SEM image of TPS-Cellulose Biocomposites

Images for TPS-Cellulose biocomposites were taken at magnifications around 1000X, 1300X, 5400X, 13500X. The images were taken to confirm the presence of cellulose nanofibers in the biocomposite. Figure 4.7 a, b and c shows the images of the TPS-Cellulose biocomposites.

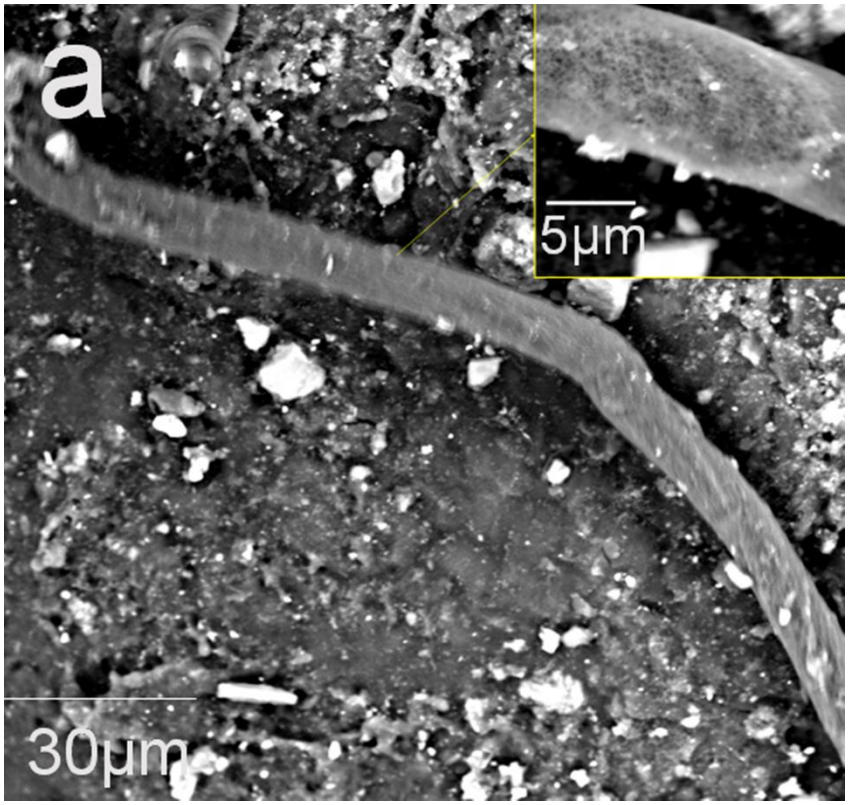

Figure 4.7 (a) : SEM images for TPS-Cellulose with volume fraction of 0.2.

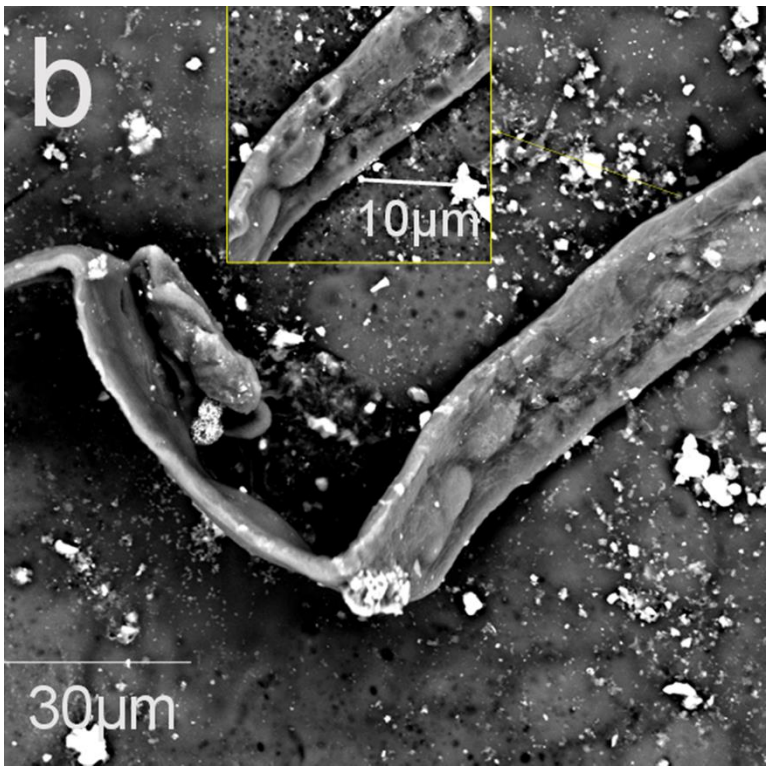

Figure 4.7 (b) : SEM images for TPS-Cellulose with volume fraction of 0.3.

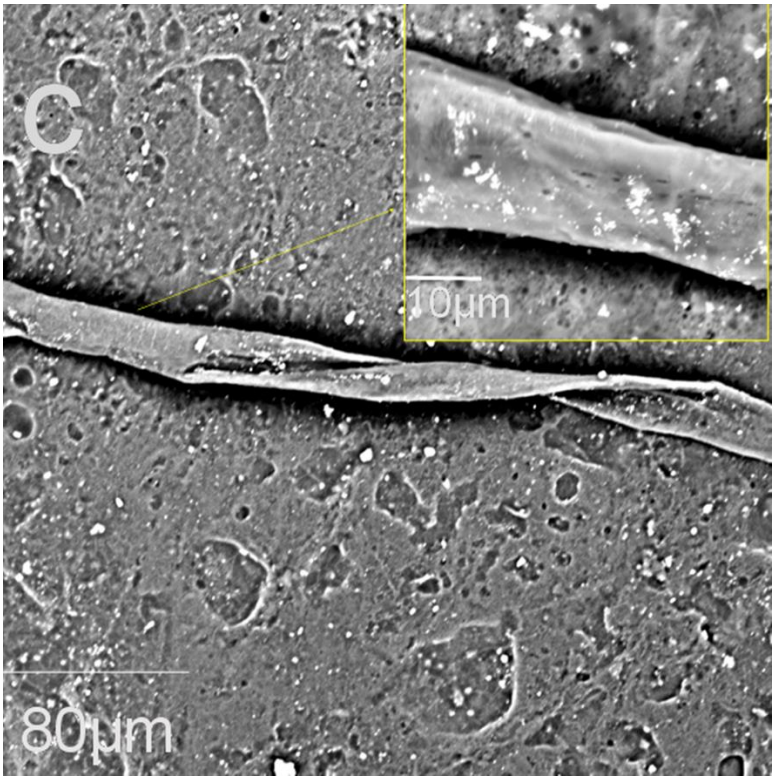

Figure 4.7(c) : SEM images for TPS-Cellulose with volume fraction of 0.5.

The microstructural images of TPS-cellulose biocomposites showed indicated that the cellulose nanofibers were successfully introduced into the TPS matrix. The SEM micrographs in figure 4.7 a,b and c shows the strong interfacial adhesion between the cellulose nanofibers and the TPS matrix.

4.1.3 Energy Dispersive X-ray spectroscopy

EDX provides the information regarding elemental percentage present in the various samples being analysed. The information is represented in percentage-wise to give an idea of the percentage of each element that makes up the sample. EDX analysis was done for TPS only, cellulose nanofibers and TPS-cellulose samples.

4.1.3.1 EDX spectroscopy for Cellulose nanofibers

Seven different spots of the SEM micrograph was selected as shown in figure 4.8a and the elemental compositions was analysed. After performing the analysis, a spectrum was generated as shown in figure 4.8b. The spectrum depicts peaks of the elements present in cellulose nanofibers.

Table 4.1 EDX elemental composition of cellulose nanofiber

Atomic number	Element symbol	Element name	Atomic concentration percentage	Weight concentration percentage	Oxide	Stoichiometric weight percentage
8	O	Oxygen	46.74	52.59		
6	C	Carbon	51.35	43.38	C	91.51
20	Ca	Calcium	0.62	1.75	Ca	3.69
11	Na	Sodium	0.71	1.15	Na	2.43
14	Si	Silicon	0.44	0.86	Si	1.81
13	Al	Aluminium	0.14	0.26	Al	0.56

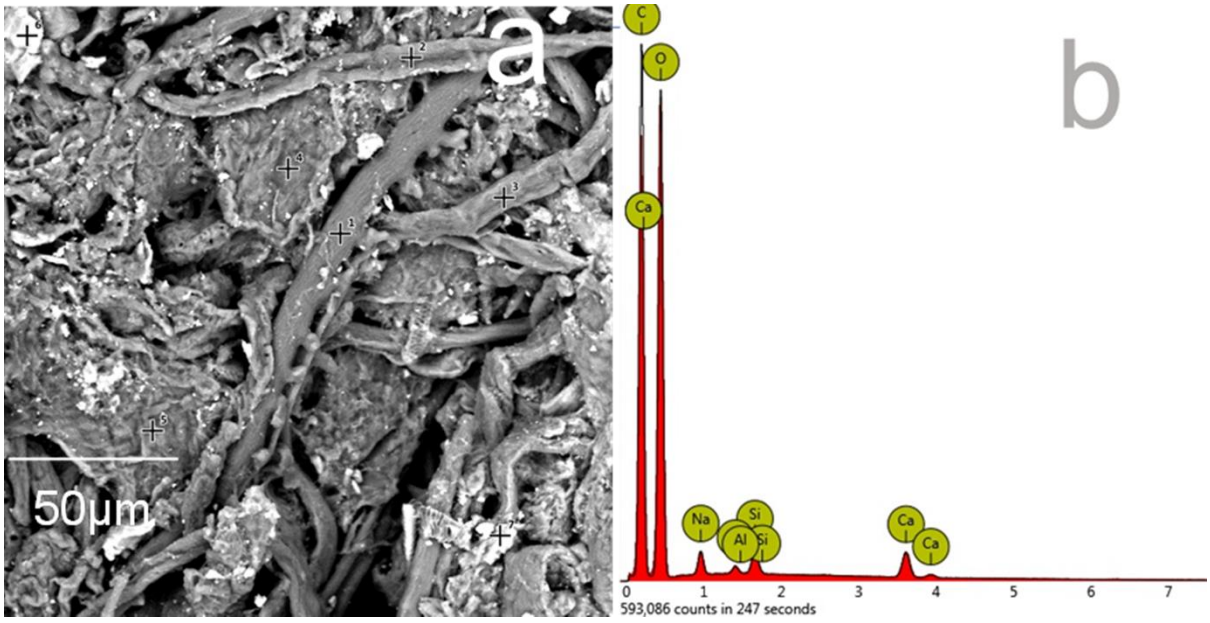

Figure 4.8 (a) EDX mapped positions on SEM micrograph, (b) EDX spectrum

The elements that were reported to be present in the cellulose nanofiber are oxygen (O), carbon (C), calcium (Ca), sodium (Na) and Silicon (Si). The elements that dominated the composition of cellulose nanofiber are oxygen and carbon, with percentage concentrations of 46.74 and 51.35 respectively. The presence of silicon, aluminium and calcium confirms that cellulose was prepared from rice husk which from literature is known to contain silicon [59], [19].

The spectrum also showed the presence Na which is assumed to be from the Sodium hydroxide used in extracting the cellulose nanofiber.

4.1.3.2 EDX spectroscopy for TPS only

The whole SEM micrograph in figure 4.9a was scanned for the elemental compositions analysis. After performing the analysis, a spectrum was generated as shown in figure 4.9b. The spectrum depicts peaks of the elements present in starch.

Table 4.2 EDX elemental composition of TPS only

Atomic number	Element symbol	Element name	Atomic concentration percentage	Weight concentration percentage	Oxide	Stoichiometric weight percentage
8	O	Oxygen	46.95	54.1		
6	C	Carbon	53.05	45.9	C	100

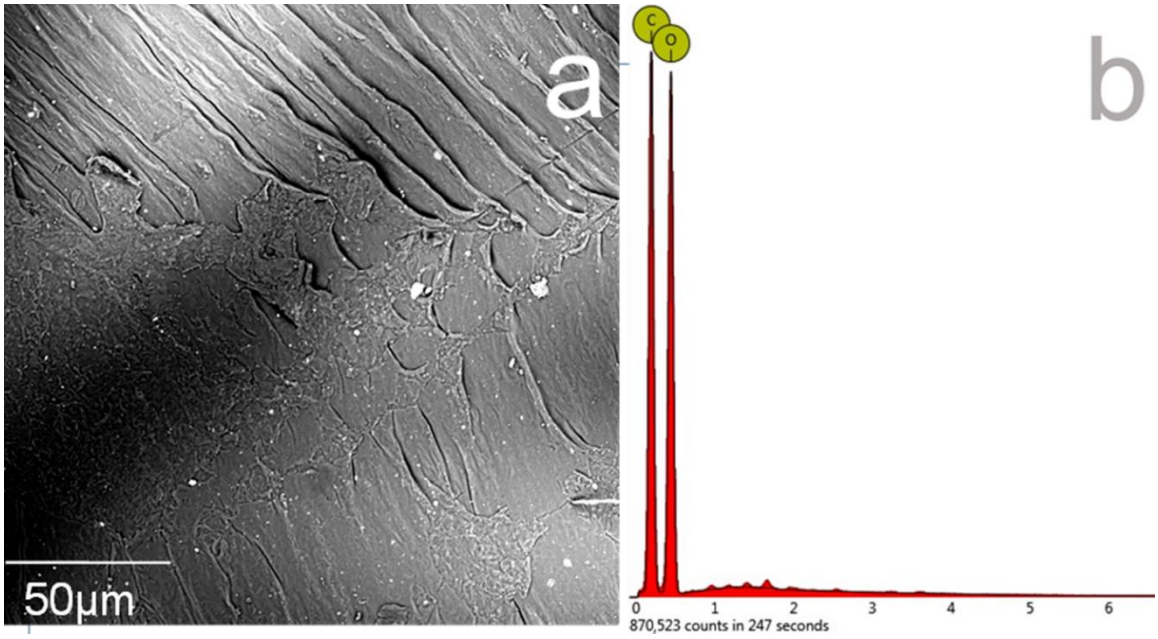

Figure 4.9 (a) SEM micrograph scanned, (b) EDX spectrum

The EDX analysis of the starch sample confirmed that starch and glycerol is made up mainly of carbon and oxygen.

4.1.3.3 EDX spectroscopy for TPS-nanokaolin

The whole SEM micrograph in figure 4.10a was scanned for the elemental compositions analysis. After performing the analysis, a spectrum was generated as shown in figure 4.10b. The spectrum depicts peaks of the elements present in cellulose nanofibers.

Table 4.3 EDX elemental composition of TPS-nanokaolin biocomposite

Atomic number	Element symbol	Element name	Atomic concentration percentage	Weight concentration percentage	Oxide	Stoichiometric weight percentage
8	O	Oxygen	45.72	51.96		
6	C	Carbon	52.72	44.98	C	93.62
14	Si	Silicon	0.95	1.9	Si	3.96
13	Al	Aluminium	0.61	1.16	Al	2.42

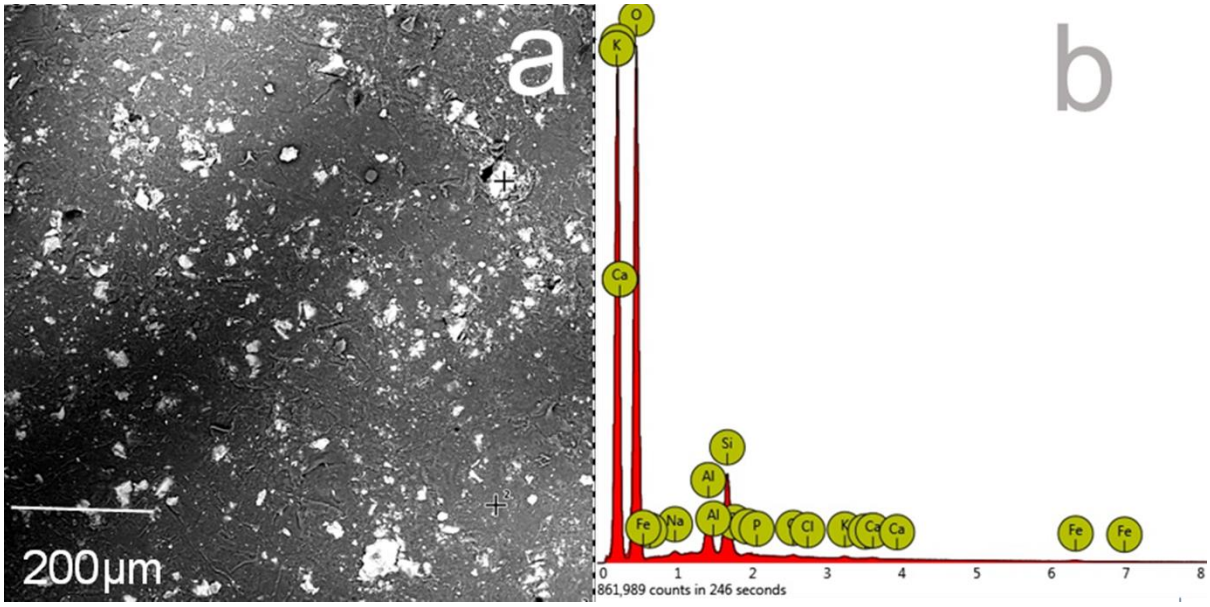

Figure 4.10 (a) SEM micrograph scanned, (b) EDX spectrum

EDX provides elemental percentage of atom for TPS-nanokaolin biocomposite film. It contains carbon 52.72%, oxygen 45.72%, aluminium 0.61% and silicon 0.95%. With the presence of silicon and aluminium, it can be said that nanokaolin was successfully utilized to obtain TPS-nanokaolin biocomposite film.

4.1.4 X-Ray Diffraction Analysis (XRD)

Figure 4.11 and 4.12 are the graphs for XRD analysis of TPS only and TPS-nanokaolin biocomposites respectively.

From the XRD results, the various representations of the peaks recorded on the diffractogram are indexed. Also, degree of crystallinity is estimated for TPS only biocomposites which is seen from figure 4.11 to be a semi-crystalline material. The degree of crystallinity is calculated from equation 4.1.

$$X_c = \frac{I_c}{I_c + I_a} * 100\% \quad \text{.....4.1}$$

Where X_c is the degree of crystallinity, I_c is the intensity of the highest diffraction peak of the crystalline phases and I_a is the Intensity of the highest peak of amorphous phase. The degree of crystallinity confirmed the introduction of nanokaolin in different volume fractions. XRD patterns also matched phases known to be nanokaolin and quartz.

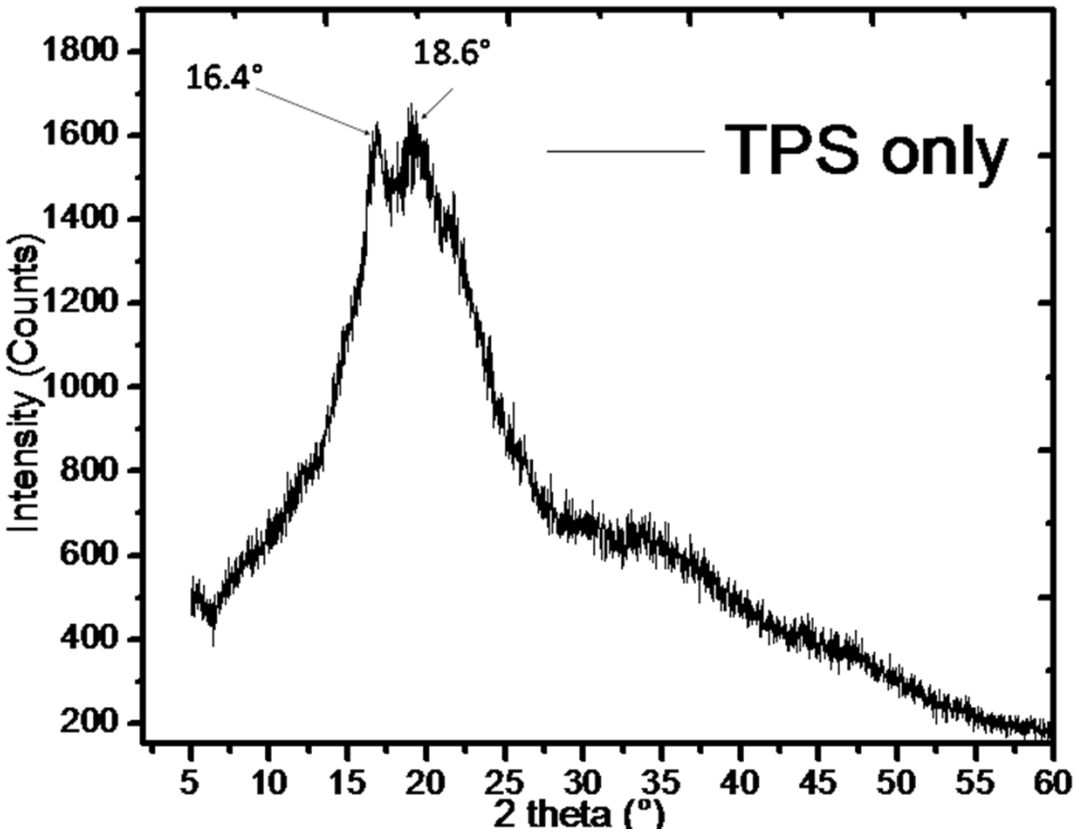

Figure 4.11 XRD pattern for TPS only biocomposite.

Figure 4.11 shows the diffractogram for TPS-only biocomposites. It was representative of a semi-crystalline material showing some crystalline peaks at 2-theta values of about 16.4° and 18.6° and the background depicting an amorphous material. The strong reflection at 2-theta value of 16.4° is characteristic of starch type known as polymorphic C [34] and the reflection at 18.6° is characteristic of starch type A and B [41].

The degree of crystallinity for TPS only biocomposite was estimated to be 53.70%.

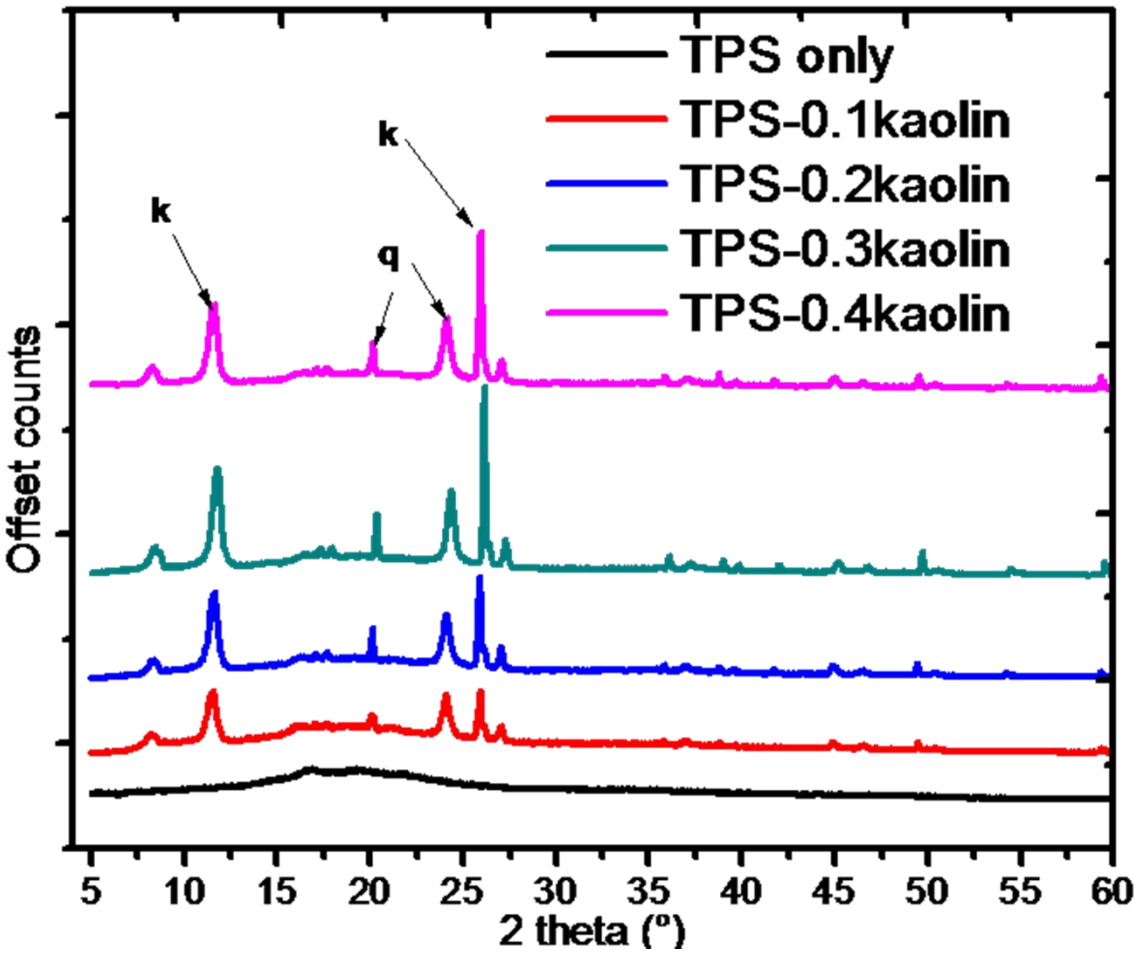

Figure 4.12 XRD patterns for TPS-nanokaolin biocomposite.

The diffractogram of the various biocomposites were analysed to study the representation of the peaks and also to study the effect on different loading of nanokaolin on the crystallinity. The two components that are usually present in nanokaolin are quartz and kaolin phases. The XRD pattern of TPS-nanokaolin biocomposite showed the characteristic crystalline peak of nanokaolin at about 11.68°, 20.05°, 24.10° and 25.99°. The rays at 2-theta values of 11.59° and 25.99° are representative of kaolin phases present in the biocomposite reinforced with nanokaolin whiles the rays at 2-theta values of 20.05° and 24.10° are representative of quartz phases. It is noticed that there are shift in the peaks of the kaolin and quartz phases in the biocomposites. The characteristic rays for kaolin are usually found at 2-theta values of 12.42°

and 24.71° whiles the characteristic rays for quartz are found at 2-theta values of 20.69° and 26.67°.

From the XRD pattern, it is noticed that varying nanokaolin volume fractions from 0.1 to 0.4, the material is still seen to be a semi-crystalline material with the degree of crystallinity increasing as the volume fraction increases. The degree of crystallinity for TPS-nanokaolin composites were estimated as 67.78%, 81.54%, 88.45% and 89.88% for TPS-0.1Kaolin, TPS-0.2Kaolin, TPS-0.3Kaolin and TPS-0.4Kaolin biocomposites respectively. This confirm the introduction of nanokaolin which is a crystalline material into the TPS matrix.

4.2 Mechanical Properties

The mechanical properties of most fiber-reinforced composites are affected by the volume fraction and kind of interfacial adhesion between fiber and matrix. Most times also, the kind of fiber and matrix (polymer) used also affects the quality of the interfacial bonding. The effects of particulate/fiber content and surface modification on the tensile properties of the biocomposites fabricated.

Polymeric materials are mostly tested for mechanical properties using the tensile test. This was achieved by continuously measuring the force that deforms the test specimen. The test specimen was continuously elongated at constant rate of extension. Stress-strain curves were developed from the data obtained from the tensile test method. The methods reported data for the load against various time (seconds) of loading.

Other properties that were obtained from the tensile test method are tensile strength, tensile strain and modulus of elasticity. The tensile strength (equation 4.2) was then determined by dividing the force that deforms the specimen by the cross-sectional area of the specimen.

Likewise, tensile strain was obtained by using the expression in equation 4.3. The results for the tensile test is shown in figure 4.13 below.

4.2.1 Stress-strain diagrams

Stress-strain curves are used to report the behaviour of a material when it has subjected to loading. It is a graph of stress, on the vertical axis against corresponding strains on the horizontal axis.

Tensile strength (stress) = $\frac{F}{A_0}$ …… 4.2

Tensile strain = $\frac{\Delta L}{L_0} = \frac{L-L_0}{L_0}$ …… 4.3

Where F is the load applied, A_0 is the initial area of the test specimen, L is the instantaneous length of the test specimen at a particular load and time and L_0 is the gage length of the test specimen. The area of the test specimen was calculated from the width and thickness of the test specimen. Table 4.4 shows the average width, thickness, gage length (L_0), and final length (L) of the test specimen. This was calculated from the various width, thickness, gage length and final length of the individual test samples.

Table 4.4 Measured variables of test specimen

Test Specimen	Width (mm)	Thickness (mm)	Gage length (mm)	Final length (mm)
TPS only	9.37	2.69	59.13	62.32
TPS-0.1C	8.35	2.87	56.83	57.27
TPS-0.2C	9.38	2.85	57.05	59.59
TPS-0.3C	8.16	2.84	57.84	58.23
TPS-0.4C	8.77	2.94	54.51	55.64
TPS-0.5C	7.62	2.66	56.02	57.25
TPS-0.1K	9.01	2.72	58.99	62.13
TPS-0.2K	9.66	2.74	61.82	64.15
TPS-0.3K	8.32	2.49	57.11	58.63
TPS-0.4K	7.92	2.56	59.97	61.63
TPS-0.5K	9.28	2.89	58.37	59.28

The measured variables stated in table 4.4 were used in calculating the stress, strain rate, elongation, modulus of elasticity, and the length of the specimen at a particular load and time (sec).

In order to calculate the strain, the individual length (L) at a particular load was required. This was calculated from the strain rate expression (equation 4.4).

Strain rate $(\dot{\varepsilon}) = \frac{L - L_0}{t * L_0}$ …… 4.4

Where L is the instantaneous length, L_0 is the gage length, t is the time in seconds and $\dot{\varepsilon}$ is the strain rate in s^{-1}.

From the strain rate expression, we can obtain the instantaneous length (L) as shown in equation 4.5.

$L = L_0 * (\varepsilon * \dot{t} + 1)$……..... 4.5

After calculating the various length at individual loads and times, we can calculate the strain of the various materials at various loads. Results for the calculated area used in calculating the stress and the calculated strain rate is shown in table 4.5.

Table 4.5 Calculated variables of test specimen

Specimen	Area (mm^2)	Strain rate (s^{-1})
TPS only	25.2427	1.079E-3
TPS-0.1C	23.8889	2.212E-4
TPS-0.2C	26.3686	1.272E-3
TPS-0.3C	23.1369	1.927E-4
TPS-0.4C	25.8407	5.923E-4
TPS-0.5C	19.8487	6.273E-4
TPS-0.1K	24.497	1.331E-3
TPS-0.2K	26.3696	8.376E-4
TPS-0.3K	20.614	5.915E-4
TPS-0.4K	20.2859	9.223E-4
TPS-0.5K	26.8808	4.469E-4

The stress strain diagrams for TPS-cellulose and TPS-nanokaolin biocomposites is reported in figure 4.13 and 4.14 respectively. It is a graph of stress on the vertical axis against strain on the horizontal axis. The diagram gives a representation of the biocomposites response to tensile loading. From the graph, we can observe the samples which are more plastic and those that are more elastic. Also, the yield strength, ultimate tensile strength and the fracture strength are determined from the stress-strain curves. The yield strength of the various composites were determined using an offset strain 0f 0.2%. From the graphs, it is noticed that most of the biocomposites do not undergo necking. It is realised that almost all the biocomposites tested had their ultimate tensile strength and the fracture strength occurring at the same value. Of all

the biocomposites, TPS only, TPS-0.1kaolin, TPS-0.5kaolin and TPS-0.2cellulose biocomposites are seen to undergo some degree of necking but is very minimal. Due to the degree of necking that these biocomposites undergo, they can be referred as ductile materials whiles the remaining biocomposites that do not undergo necking can be referred as brittle materials.

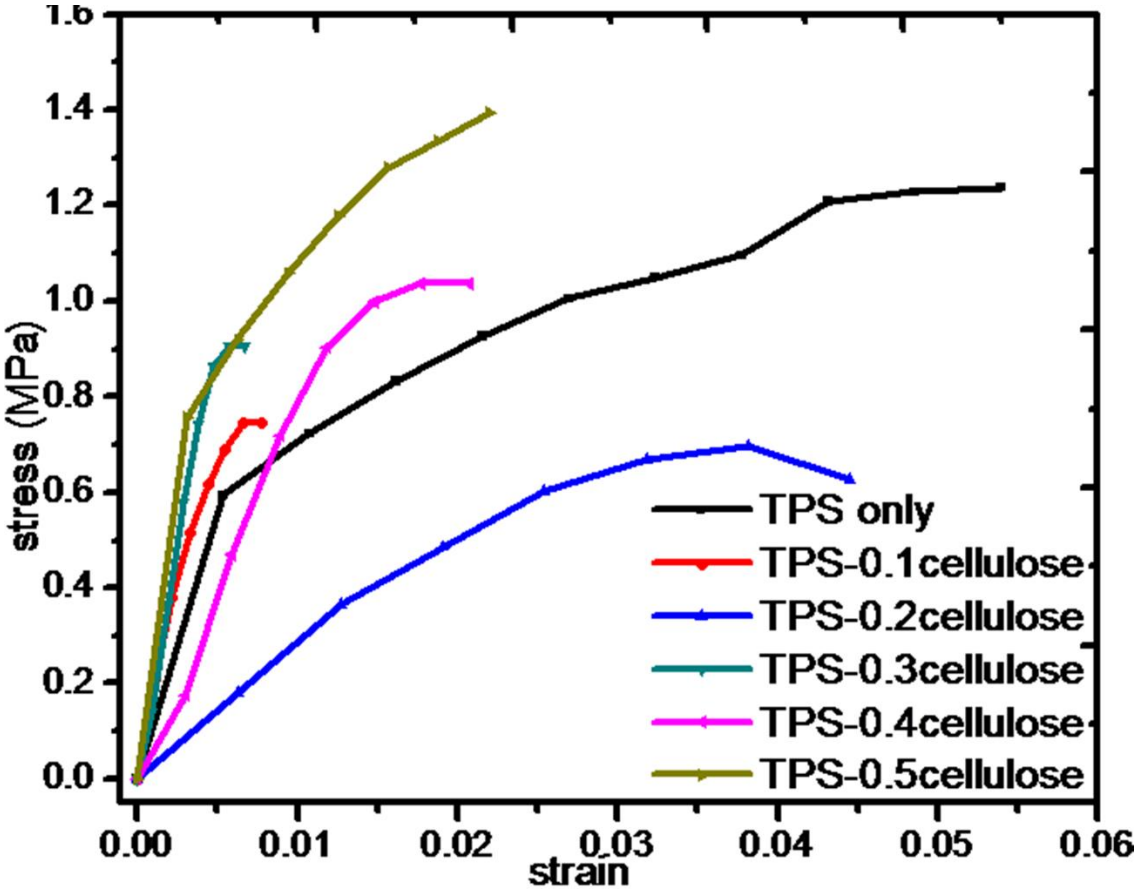

Figure 4.13 Stress-strain curves for TPS-Cellulose biocomposites

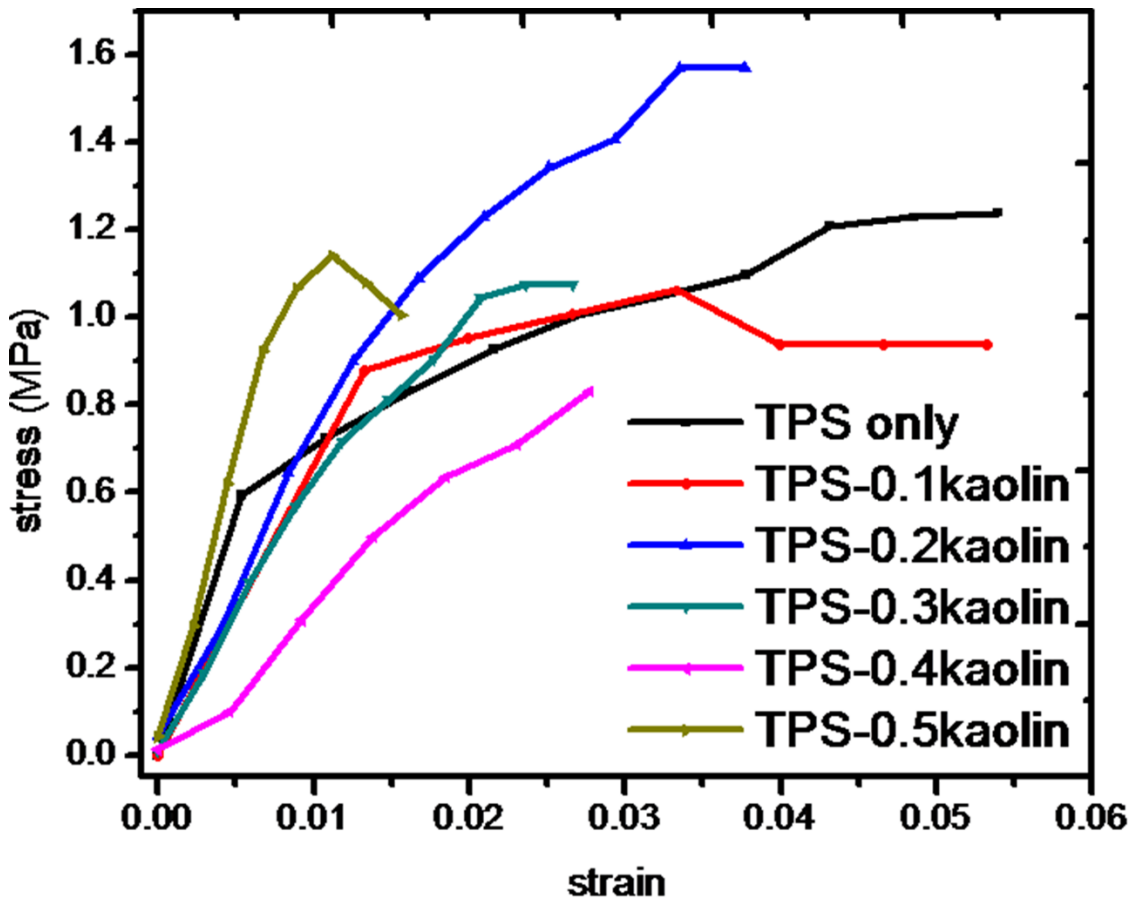

Figure 4.14 Stress-strain curves for TPS-nanokaolin biocomposites

4.2.2 Yield Strength

The results for the yield strength was determined from the stress-strain graphs shown in figures 4.13 and 4.14. This is the strength at which a specific amount of plastic deformation begins to occur. The graph for the yield strength is reported in figure 4.15. This is a graph of reinforcement content against the yield strength.

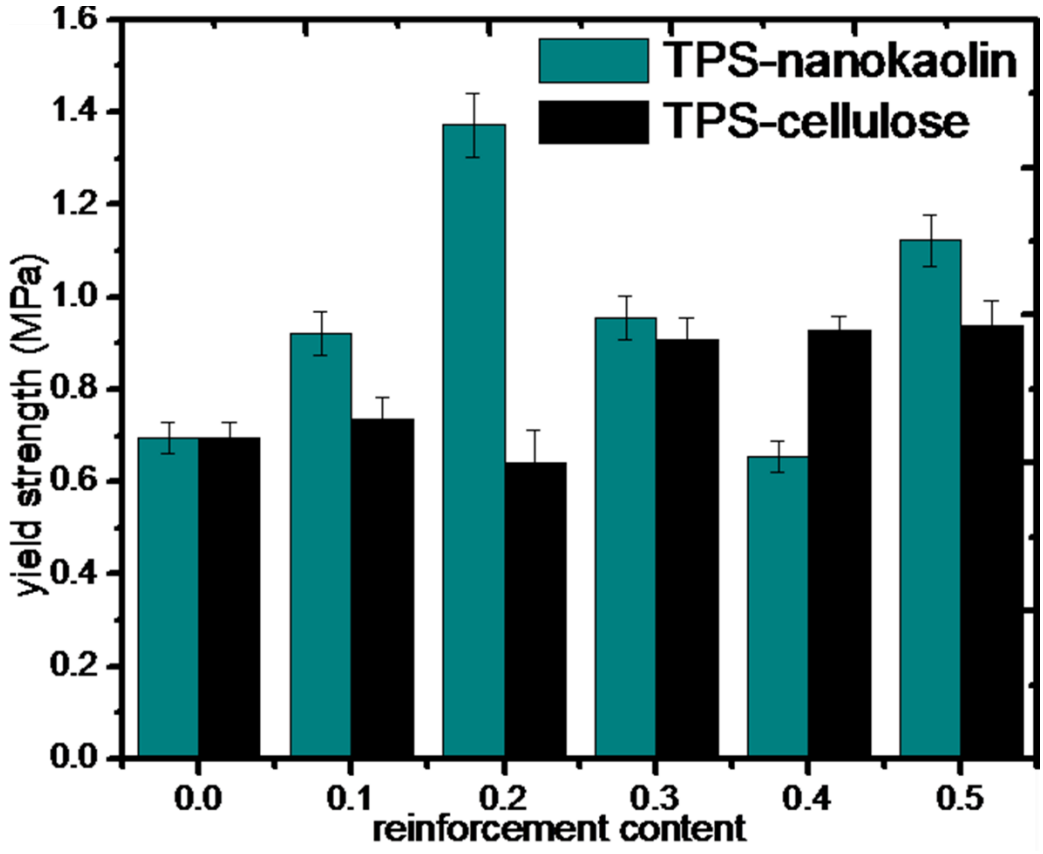

Figure 4.15 Yield strength for nanokaolin and cellulose nanofiber biocomposition.

From figure 4.15, the maximum yield strength reported for the TPS-kaolin biocomposites was recorded for TPS-0.2kaolin biocomposite with a value of 1.3714 MPa whiles the minimum yield strength was recorded for TPS-0.4kaolin biocomposite. The average yield strength recorded for TPS-kaolin biocomposites was determined to be 1.0054 MPa. As the volume fraction of the nanoclay is increased, the yield strength increases. This was consistent and followed a finding reported by Chris DeArmitt, which stated that adding fillers with high aspect ratio such as nanoclay and glass fiber increases the yield strength [12]. However, the adhesion of the polymer and nanoclay interphase is compromised when the volume fraction of the nanoclay increases beyond 0.2.

For TPS-cellulose biocomposites, the maximum yield strength was recorded for TPS-0.5cellulose biocomposite with value 0.9367 MPa whiles the minimum yield strength was

recorded for TPS-0.2cellulose biocomposite with value 0.6421 MPA. The average yield strength for TPS-cellulose biocomposites was determined to be 0.8299 MPa. As the volume fraction of the cellulose is increased from 0.2 to 0.5, the yield strength increases. At these volume fractions the interaction of the cellulose and the starch polymer is seen to be very good as reported in the SEM micrographs.

4.2.3 Ultimate Tensile Strength (UTS)

From the stress-strain diagrams of TPS-cellulose and TPS-kaolin biocomposites shown in figure 4.13 and 4.14, the maximum point on the curve is termed to be the ultimate tensile strength. The ultimate tensile strength for the biocomposites is reported in figure 4.16. It is a graph of reinforcement content against the ultimate tensile strength.

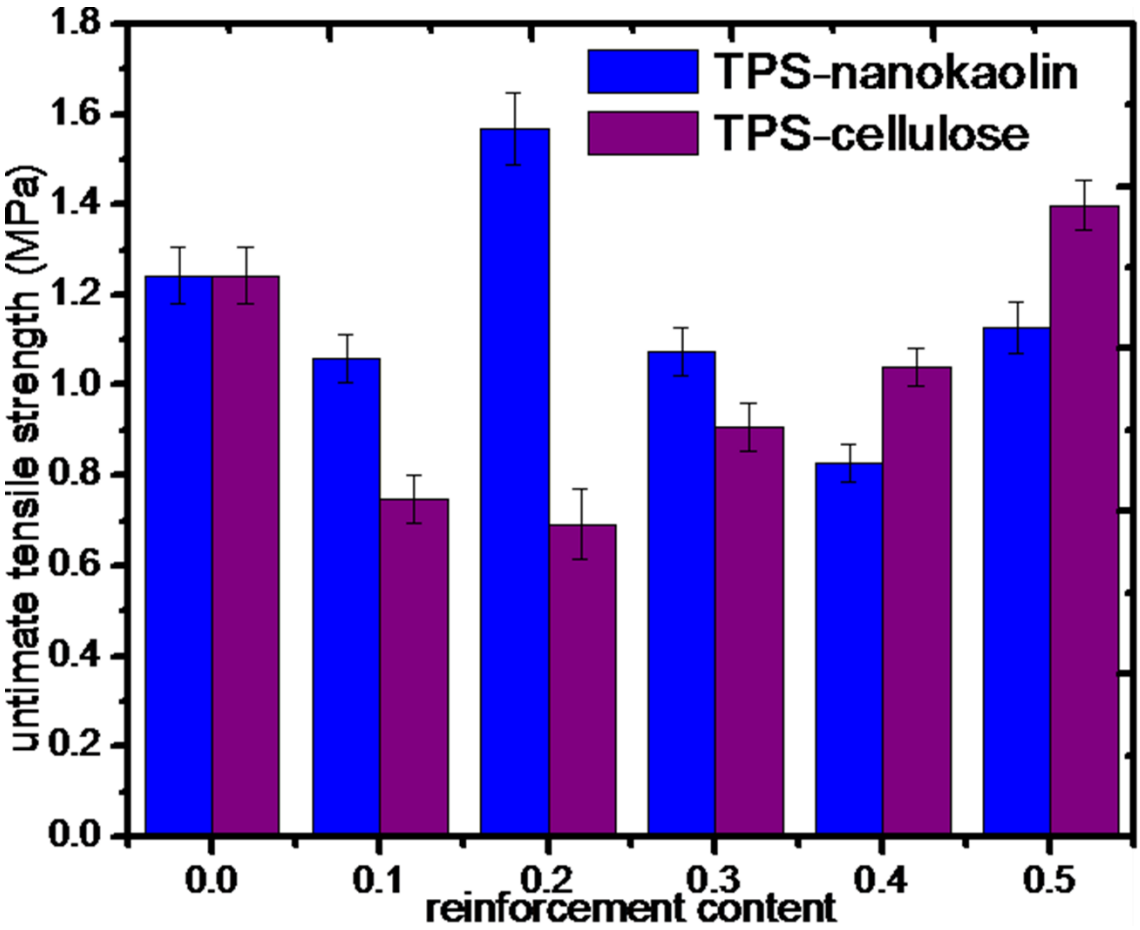

Figure 4.16 UTS for nanokaolin and cellulose modified biocomposition.

For TPS-kaolin biocomposites, the maximum UTS was recorded for TPS-0.2kaolin biocomposite with value 1.5674 MPa whiles the minimum UTS was recorded for TPS-0.4kaolin biocomposite with value 0.8264 MPa. The average UTS was recorded to be 1.13098 MPA.

With the interaction effect of nanoclay and starch polymer being affected as the volume fraction increases, the UTS is seen to decrease as the volume fraction increases beyond 0.2. similar to the trend reported for the yield strength, it is seen that as the volume fraction of nanoclay increases, from 0.2 to 0.5, the interphase bonding between the nanoclay and the starch polymer is minimal, hence affecting the strength.

For TPS-cellulose biocomposites, the maximum UTS was recorded for TPS-0.5cellulose biocomposite with value 1.3978 MPa whiles the minimum UTS was recorded for TPS-0.2cellulose biocomposite with value 0.6928 MPA. The average UTS for TPS-cellulose biocomposites was determined to be 0.9569 MPa. The trend is similar to that obtained for the yield strength. Most materials have their UTS similar to the fracture strength which is reported next.

4.2.4 Fracture Strength

Fracture strength or breaking strength is the strength at which the specimen fails or breaks. At this point, the mechanical strength of the specimen can be determined. Most times, the fracture strength is taken to be the mechanical strength, and this is because, it gives an information of the strength at which the material breaks.

The results for the fracture strength of TPS-cellulose and TPS-kaolin biocomposites are reported in figure 4.17. It is reported as a graph of reinforcement content against the fracture strength.

For TPS-kaolin biocomposite, the maximum fracture strength is recorded for TPS-0.2kaolin biocomposite with value 1.5674 MPa whiles the minimum fracture strength was recorded for TPS-0.4kaolin biocomposite with value 0.8264 MPa. The average fracture strength was determined to be 1.07996 MPa.

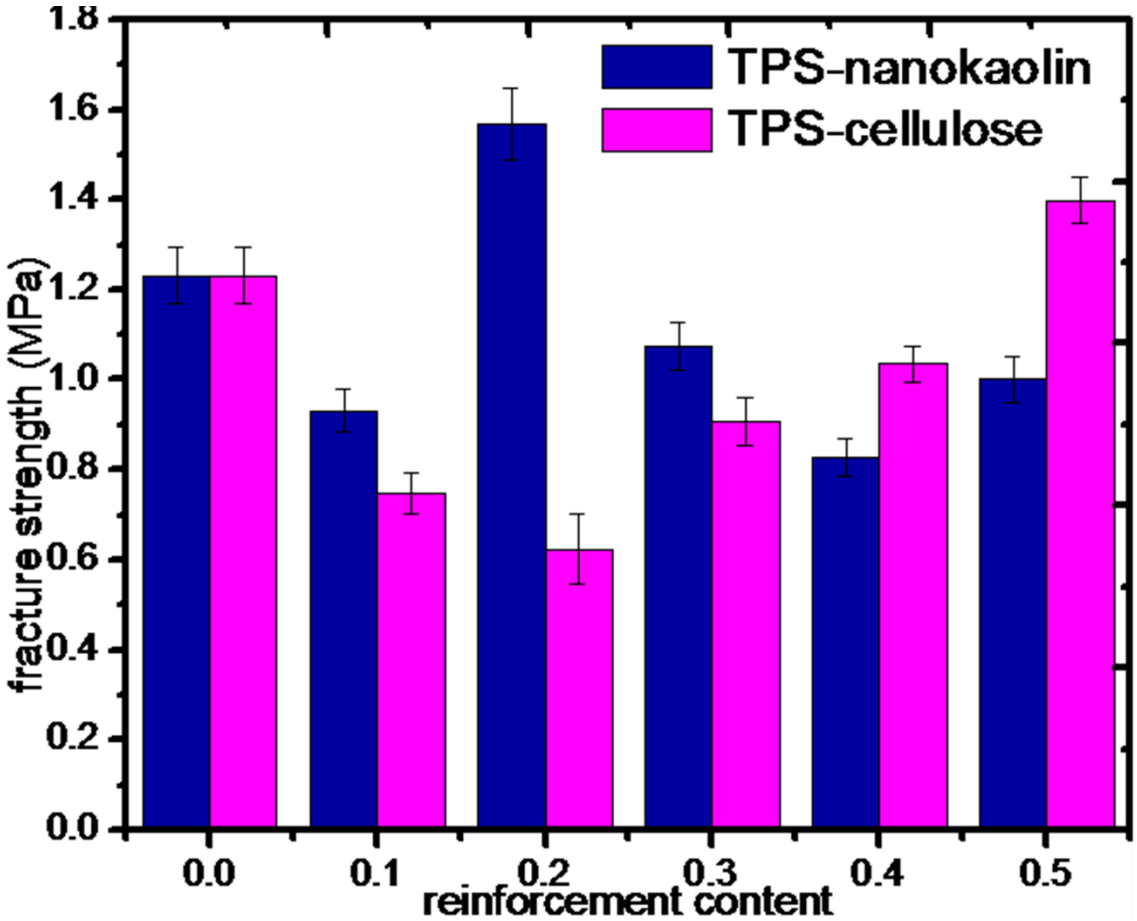

Figure 4.17 Young's Modulus for nanokaolin and cellulose modified biocomposite

The trend for the fracture strength is similar to that for the yield strength and the ultimate tensile strength. TPS-0.2kaolin biocomposite is seen to show higher fracture strength due to the good interphase bonding between the nanoclay and the starch polymer at lower volume fractions.

Similarly, TPS-0.4kaolin biocomposite shows low fracture strength, meaning at higher volume fractions, there is poor interphase bonding between the nanoclay and the starch polymer.

TPS-cellulose biocomposites follow the same trend reported for yield strength and UTS results.

The improvements in the strength (fracture strength, yield strength and the ultimate tensile strength) is as a result of the high aspect ratio of the nanoclay and the cellulose used as modifiers in the biocomposite preparation. Also, it can be explained that, whenever there is better interaction between the nanoclay-starch and cellulose-starch interphase, the strength is improved. In all the determined strengths, it is noticed that TPS-0.4kaolin showed poor strength. And this is because at such high volume fraction of nanoclay, there is higher possibility of clay particle agglomeration, hence clay-clay interphase which creates stress concentration sites and weakens the biocomposite [33]. Similarly, for TPS-0.2cellulose, at lower volume fractions of cellulose whiskers, the aspect ratio is very low hence a high possibility of starch-starch interphase reaction which weakens the composites [6]. These assumptions are confirmed by the SEM morphology of the biocomposites shown from figure 4.4 to figure 4.7.

4.3 Water Vapour Permeability Test

These tests were conducted on the sample to report on the reaction of the sample to chemical attack which is very crucial to packaging application.

The weight recordings for the specimen was used to calculate for the water vapour permeability and transmission (equation 4.6).

$$WVTR = \frac{G}{tA} \quad \text{.....4.6}$$

Where ‘G’ is the change weight of the specimen to be tested, ‘t’ is the time at which the weight change occurs and ‘A’ is the area of the specimen. Water vapour transmission rate results are reported in table 4.6 and figure 4.18 for TPS-nanokaolin biocomposite whiles for TPS-cellulose biocomposites, the results are reported in table 4.7 and figure 4.19.

For TPS-nanokaolin and TPS-cellulose biocomposites, the test samples of recorded weight M1 were kept in the desiccator for one day and the final weight recorded as M2. The area of the

specimen was calculated from the specimen diameter, which was recorded as 0.0567m for both TPS-nanokaolin and TPS-Cellulose biocomposites.

Table 4.6 Water vapour transmission rate test for TPS-nanokaolin biocomposites.

Sample	M1/g	M2/g	WVTR/(g/m.day)
Control	19.58	18.977	238.7839
0.1	26.46	25.954	200.3725
0.2	27.12	26.622	197.2046
0.3	26.068	25.62	177.4049
0.4	24.058	23.483	227.6961
0.5	22.678	22.089	233.24

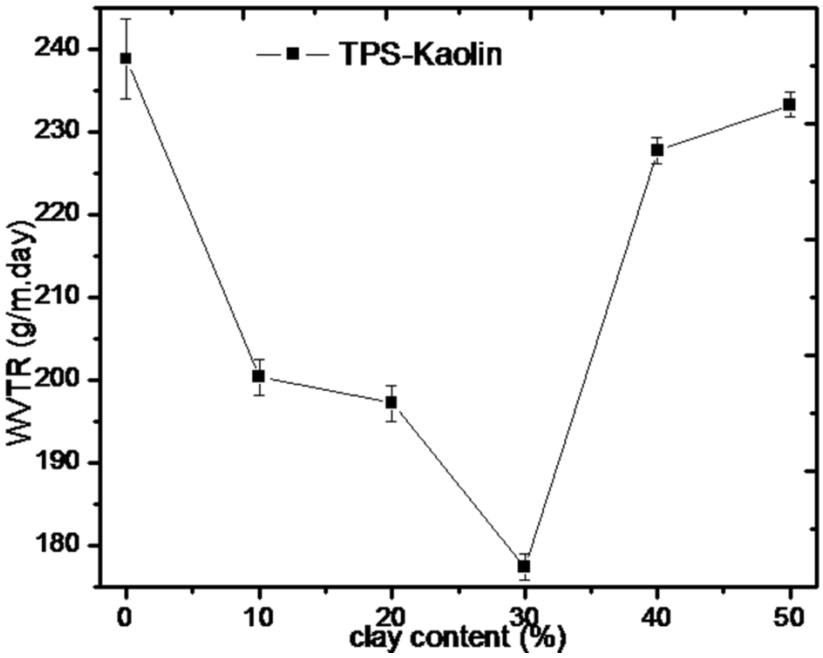

Figure 4.18 Water Vapor Transmission Rate for TPS-nanokaolin biocomposites.

The results shown in figure 4.18 for TPS-nanokaolin biocomposites shows the reduction in the water vapour transmission rate as the content of the clay increases to 0.3. After which the water vapour transmission rate increases but still better than that of the control sample. The results show that the rate of water vapour transmission can be as low as 171.81 g/m.day for clay

content of 0.3 vf. Control sample was shown to allow water vapour though it at a faster rate of 386.57 g/m.day.

According to an article by Polyprint, water vapour transmission rate can be affected by the orientation of the crystals present in the biocomposites [53]. With starch showing an alternating layer of Crystalline and amorphous phases, adding nanokaolin which has a crystal structure of triclinic.

With the amount of nanokaolin increasing in the sample, the crystallinity increases hence the water vapour transmission rate is improved. However, at nanokaolin percentage content of 0.4, it is assumed that that the crystals are more aligned in similar directions hence allows more moisture to go through the film.

Table 4.7 Water vapour transmission rate test for TPS-cellulose biocomposites.

Sample	M1/g	M2/g	WVTR/(g/m.day)
0	19.58	18.977	238.7839
10	31.67	31.397	108.1061
20	26.701	26.431	106.9182
30	30.407	30.203	80.78261
40	29.899	29.698	79.59463
50	30.794	30.606	74.44672

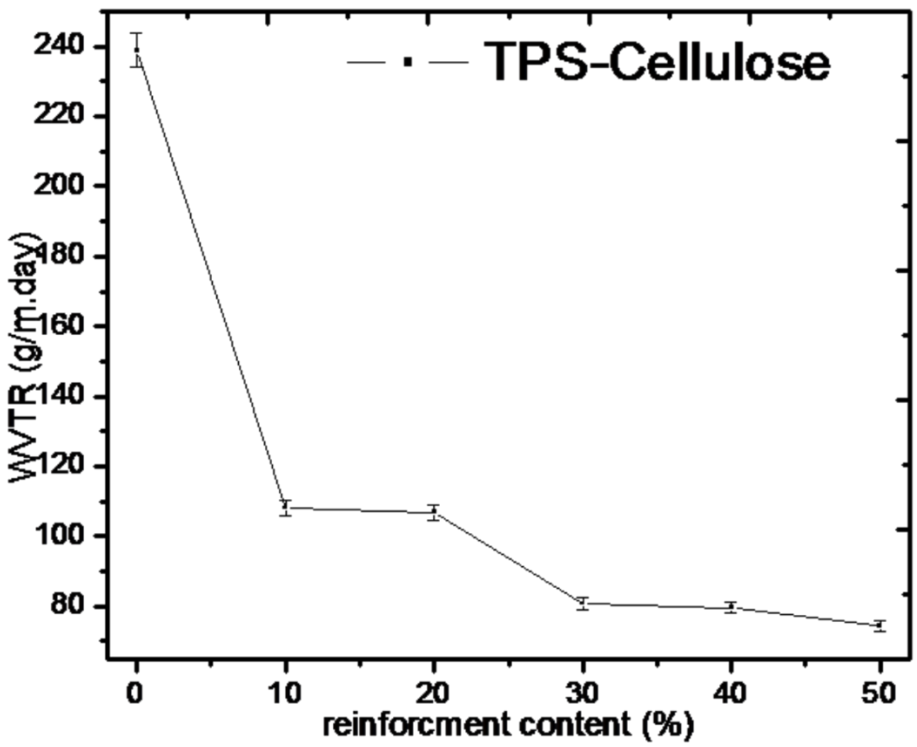

Figure 4.19 Water Vapor Transmission Rate for TPS-cellulose biocomposites.

The results shown in figure 4.19 for TPS-cellulose biocomposites shows that as the cellulose content increases, the water vapour transmission decreases. The material with no cellulose content was noticed to have high water vapour transmission rate of 238.7839 g/m.day whiles biocomposite with cellulose volume fraction of 0.5 allowed less amount of water vapour to transmit through. TPS-cellulose biocomposite with cellulose volume fraction of 0.5 gave water vapour transmission rate of 74.4467 g/m.day.

From the trend, it can be stated that as the volume fraction of cellulose increases in the biocomposite, the materials develops a high barrier to transmission of water vapour. This can be explained based on the principle of hydrophilic nature of starch and the hygroscopic nature of the cellulose nanofibers. As the cellulose content in the biocomposite increases, the starch content also tends to be decreasing. The dispersed phase of cellulose nanofibers elongates the water particle part, hence the biocomposite absorbs less water but repels more water [49]. This creates the barrier in biocomposites modified with cellulose in different volume fractions.

4.4 Thermal Properties of Biocomposites

For TGA technique, the response of the biocomposites to temperature changes is reported in figure 4.20 for TPS-kaolin biocomposites and figure 4.21 for TPS-cellulose biocomposites.

In the figure 4.20, we see that there is change is mass of the various samples with the changes in temperature. For nanokaolin only thermographs, there is mass loss recorded in temperature range of 450-600°C. The total mass loss observed for nanokaolin only was seen to be around 7.5%.

The thermograms of TPS-kaolin biocomposites shows four regions of mass loss. The first one is between 60°C and 180°C corresponding to water loss, the second between 180°C and 240°C corresponding to evaporation of the glycerol, the third one between 305°C and 358°C corresponding to starch decomposition and the last one between 360°C and 600°C corresponding to the dehydrolisation of the silicates of nanokaolin.

The addition of nanokaolin into the starch matrix was seen to enhance the thermal stability of the composite. It was seen that as the volume fraction of the nanoclay increases from 0 to 0.5, the mass loss was reduced. In the biocomposite, nanokaolin acts as a heat barrier which improves the general thermal stability of the system.

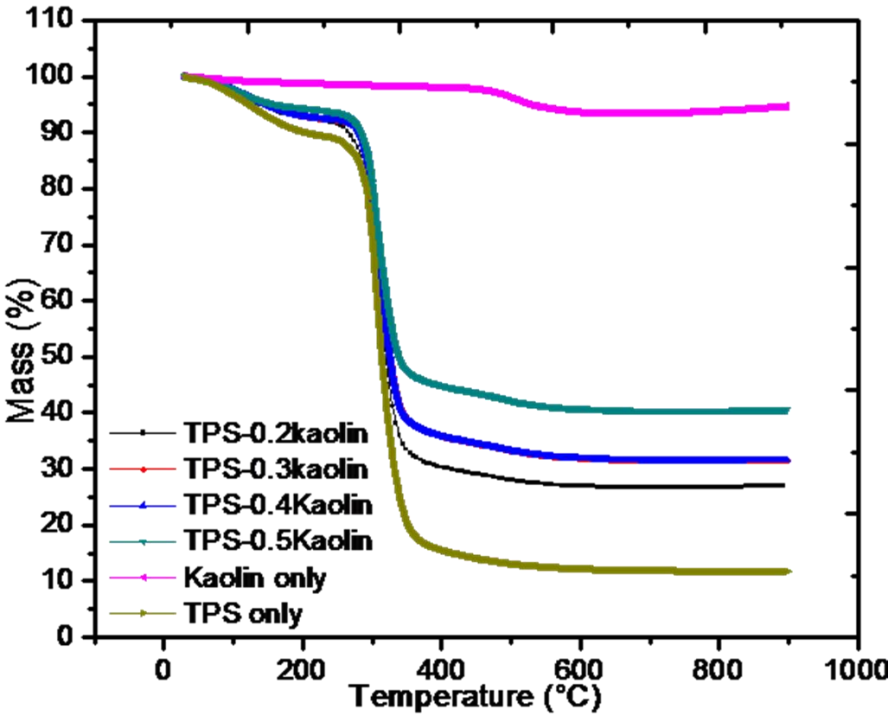

Figure 4.20 Thermograms of nanokaolin only, TPS only and TPS-kaolin biocomposite

The thermograms for TPS-cellulose biocomposites as shown in figure 4.21, shows three regions. The first one is between 60°C and 230°C corresponding to water loss and evaporation of glycerol, the second between 257°C and 370°C corresponding to the decomposition of starch and the third one between 370°C and 665°C corresponding to the decomposition of cellulose fiber structures. It is noted that the biocomposite modified with 0.4 volume fraction of cellulose nanofiber is the most stable amongst the other TPS-cellulose biocomposites.

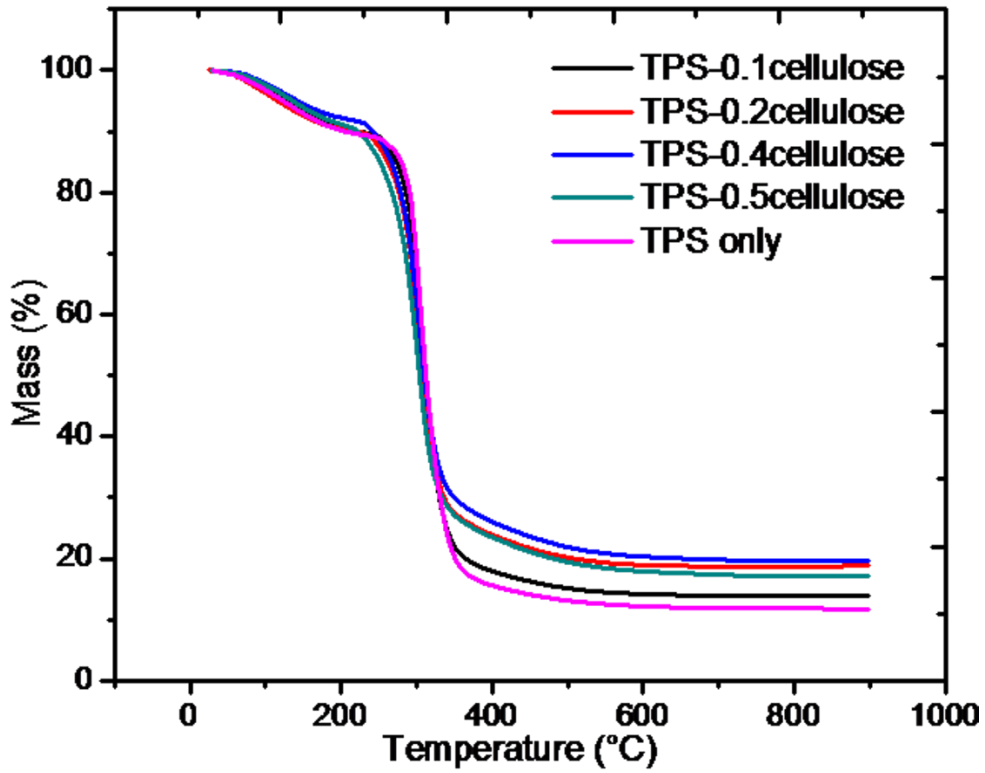

Figure 4.21 Thermograms of TPS only and TPS-cellulose biocomposite

Differential Scanning Calorimetry (DSC) were performed on samples of mass ranges between 10 and 18 mg. The samples were heated from *1*0°C to 240°C at a heating rate of 5°C/min.

The results for TPS-kaolin biocomposites is shown in figure 4.22 and that for TPS-cellulose biocomposite is shown in figure 4.23.

The results show that TPS only biocomposites gives an endothermic peak starting at 59.8°C and the peak temperature at 100.7°C. The results for nanokaolin only also showed an exothermic peak starting at 52.9°C and the peak at 76.9°C. It is noticed from figure 4.22 that as the volume fraction of nanokaolin is increased, the endothermic peak is reached at towards lower temperatures. A major change in the energy involved is also observed. For TPS only, the energy absorbed is about 0.399mW/mg. For nanokaolin only, the energy given off is about 0.084mW/mg. As the volume fraction of nanokaolin is increased, the energy absorbed by the TPS-kaolin biocomposites is reduced to 0.377mW/mg for TPS-0.1kaolin biocomposite,

0.335mW/mg for TPS-0.3kaolin biocomposite and 0.323mW/mg for TPS-0.5kaolin biocomposite.

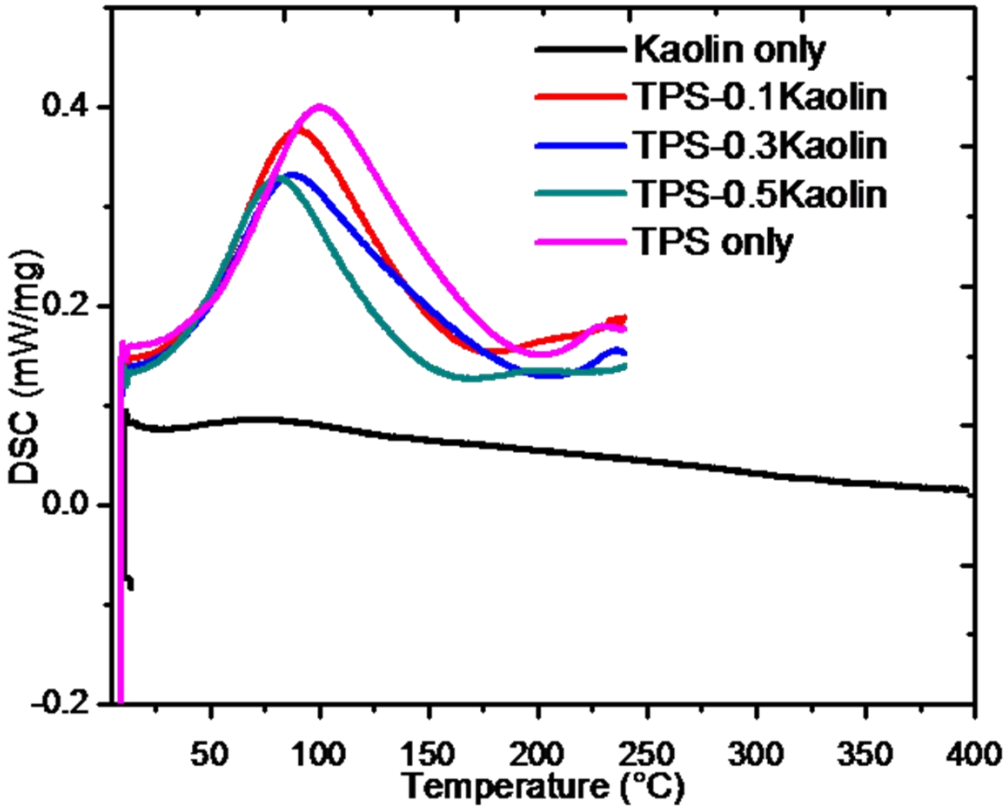

Figure 4.22 DSC curves for nanokaolin, TPS only and TPS-kaolin biocomposites

From figure 4.23, the results for cellulose nanofiber showed an endothermic peak starting at 125.6°C and the peak at 140.3°C. It is noticed that as the volume fraction of cellulose nanofiber is increased, the endothermic peak is reached at towards lower temperatures. A major change in the energy involved is also observed. For TPS only, the energy absorbed is about 0.399mW/mg. For cellulose nanofiber, the energy absorbed is about 0.711mW/mg. As the volume fraction of cellulose nanofiber is increased, the energy absorbed by the TPS-cellulose biocomposites is reduced to 0.388mW/mg for TPS-0.1cellulose biocomposite, 0.378mW/mg for TPS-0.3cellulose biocomposite and 0.357mW/mg for TPS-0.5cellulose biocomposite.

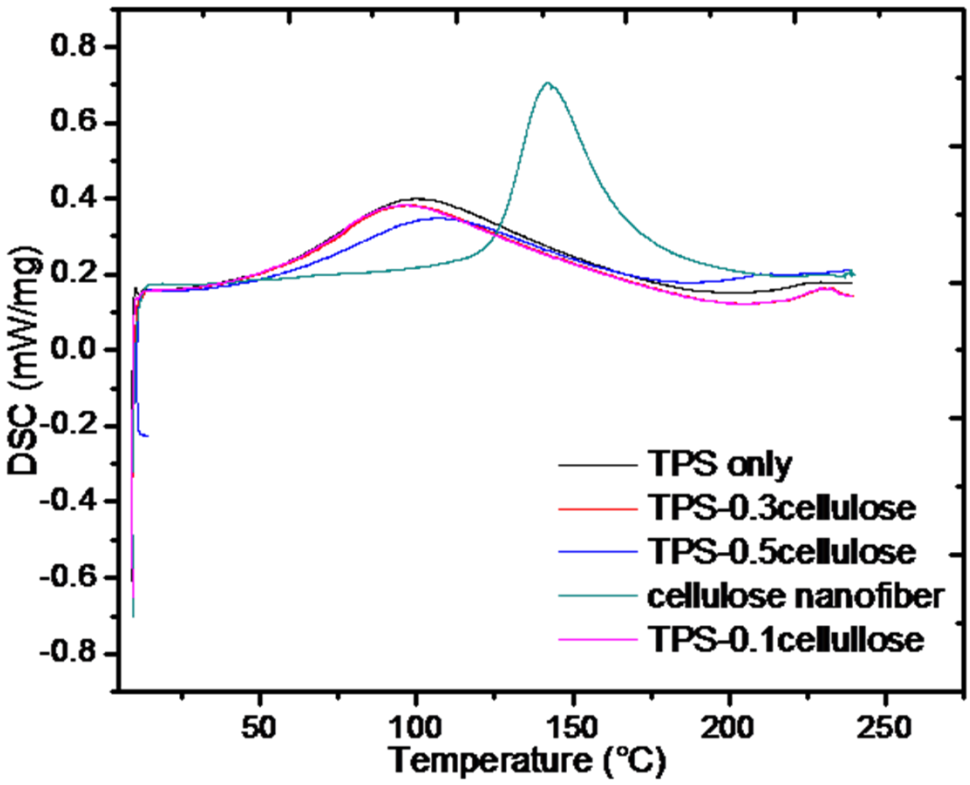

Figure 4.23 DSC curves for cellulose nanofiber, TPS only and TPS-cellulose biocomposites

4.5 Modelling of mechanical properties results

The results for the analytical and numerical modelling of the mechanical properties of the biocomposite gives a representation of the tensile loading simulated in the abaqus cae software.

The model was prepared for starch only, kaolin only, cellulose fiber only, TPS-kaolin and TPS-cellulose. The model designed were simulated to predict the response of the various materials (starch, kaolin and cellulose fiber) to tensile loading. The results confirmed the trend that was reported in the laboratory experiment. And the points at which are known as the high stress regions of the biocomposites. After simulating, it was noticed that the high stress regions of the biocomposites is seen to be at the grips of the model. And this was shown and confirmed by the experimental work. Figure 4.24 (a), (b) and (c) are the tensile test model after tensile

load is applied to the various biocomposites. This figure reports colour coding of the Von-Misses stress and the various stress values.

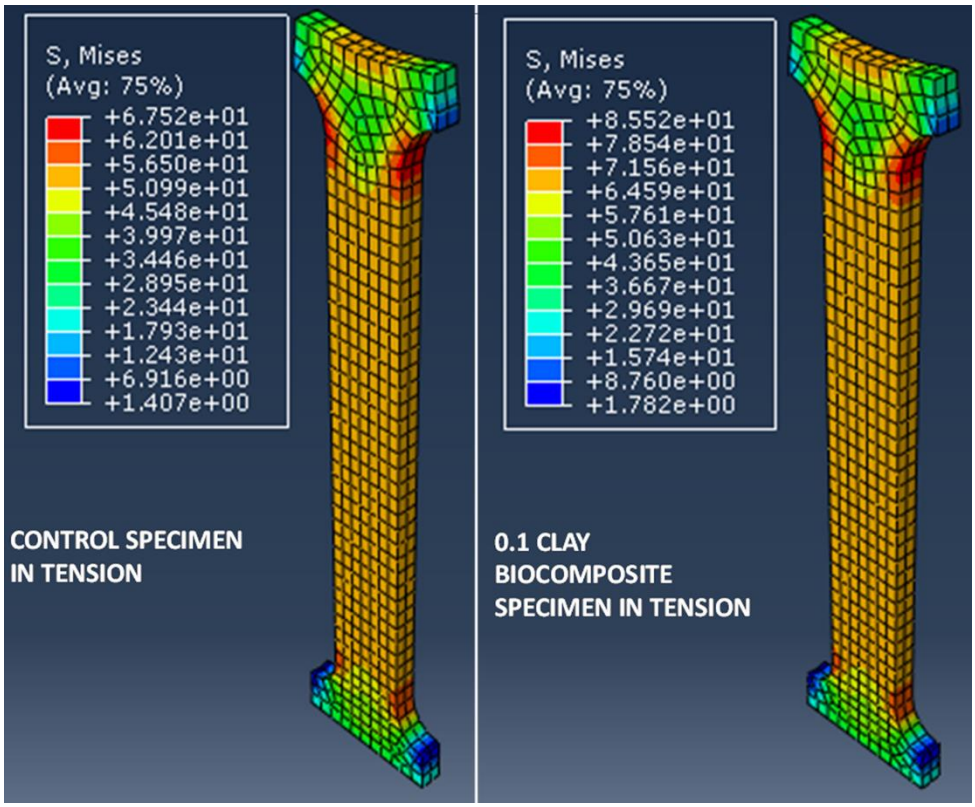

Figure 4.24 (a) : Results for tensile (bone-shape) model.

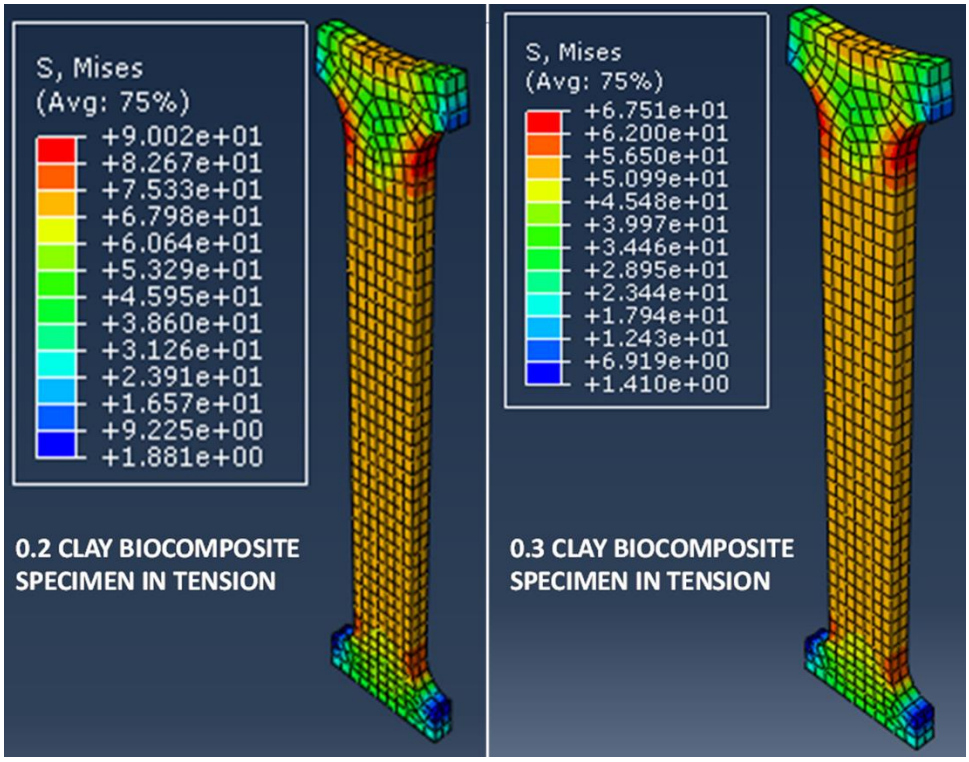

Figure 4.24 (b) : Results for tensile (bone-shape) model.

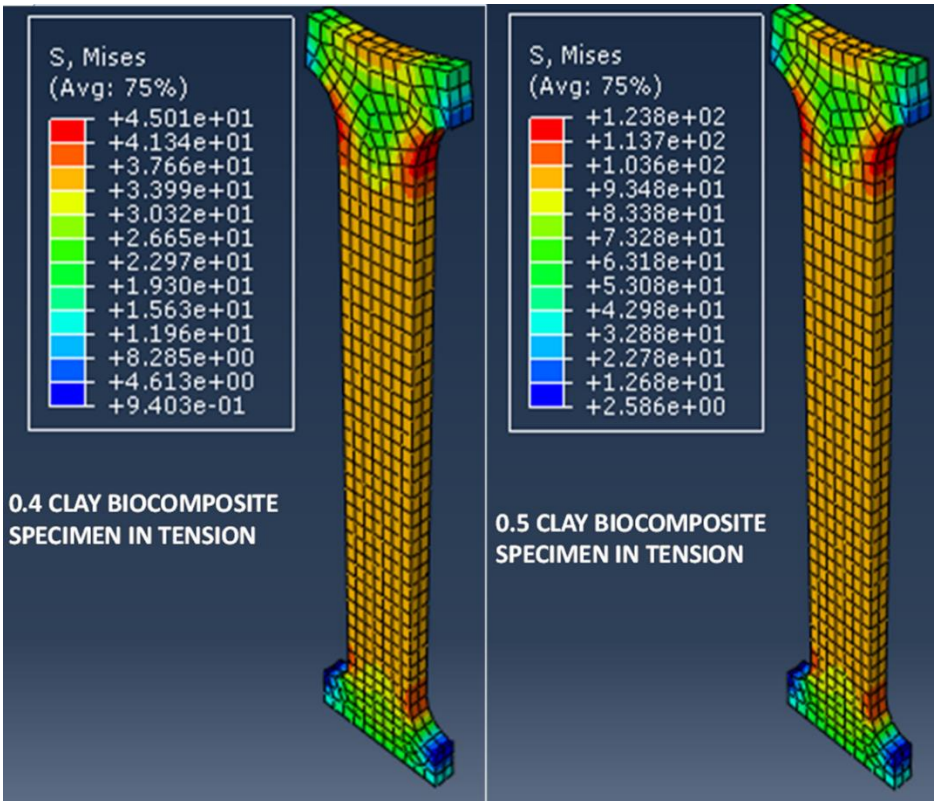

Figure 4.24(c) : Results for tensile (bone-shape) model.

CHAPTER FIVE

5.0. CONCLUSION AND RECOMMENDATION

5.1. Conclusion

With most Ghanaian consumers very ok and growing fond with packages made from plastic materials, it is having diverse effects on the environment and surroundings [1]. The menace of environmental pollution caused by the non-biodegradability of plastic packages is affecting plant, water, animal and the soil.

Fabricating biodegradable composites using natural and readily available material was the prime aim of this project. The materials that were used were mostly extracted from agricultural products, agrowaste and naanokaolin.

The fabricated biocomposites were characterised by FTIR, XRD, Tensile Test, water vapour transmission test, SEM, EDX, TGA and DSC.

FTIR was conducted to confirm the functional groups that are present in the biocomposite with the base material been starch (a carbohydrate) and also to identify and confirm the chemical bonds present in polysaccharides. The characterisation was also to confirm the presence of new chemical bonds due the fabrication process.

The FTIR spectra obtained for TPS only, TPS-nanokaolin and TPS-cellulose all showed the band for OH stretching in starch-glycerol reactions, OH bending of water molecules and CH-bending bonds. That for TPS-nanokaolin also showed the band for Si-O-C which is very characteristic of the silica phase present in nanokaolin.

The tensile test was conducted to know the response of the biocomposite fabricated to tensile forces by reporting yield strength, ultimate tensile strength and fracture strength. These parameters were obtained from the stress-strain diagram developed from the tensile test method. In all the determined strengths (yield strength, ultimate tensile strength and fracture

strength), it is noticed that TPS-0.4kaolin showed poor strength (yield strength, ultimate tensile strength and fracture strength). And this is because at such high volume fraction of nanoclay, there is higher possibility of clay particle agglomeration, hence clay-clay interphase which creates stress concentration sites and weakens the biocomposite [33]. Similarly, for TPS-0.2cellulose, at lower volume fractions of cellulose whiskers, the aspect ratio is very low hence a high possibility of starch-starch interphase reaction which weakens the composites [6].

However, to select a material based on strength, TPS-0.2kaolin has shown to depict as high as 1.5 MPa mechanical strength.

The water vapour transmission rate test was done to know the biocomposite which has the appropriate barrier to water vapour. The results showed that TPS-cellulose biocomposites with cellulose nanofiber volume fraction of 0.5 had the better water vapour barrier. That for TPS-nanokaolin biocomposite reported that biocomposite with nanokaolin volume fraction of 0.3 had good barrier to water vapour.

SEM analysis showed micrographs of the TPS-nanokaolin and TPS-cellulose biocomposites. These micrographs reported that the nanokaolin particles are uniformly distributed in the TPS matrix. And also that the cellulose nanofibers were not uniformly distributed in the biocomposites.

EDX also reported and confirmed the elemental compositions of the TPS only, TPS-nanokaolin, TPS-cellulose biocomposites and cellulose nanofibers. The elements that were reported to be present in TPS only are C, O which is known to be present because TPS was fabricated from starch (a carbohydrate) and glycerol (made up of chains of C and O). Si and Al were picked up as elements in the TPS-nanokaolin biocomposites in addition to the C and O of TPS phase. For cellulose nanofibers, the elements that were recorded are C, O, Si, Al, Ca and Na. Si and Ca are elements that are reported from literature to be in rice husk [50], [27].

Also, it is assumed that Na was as a result of traces left behind from the extraction of cellulose nanofiber.

XRD analysis was also done to show the crystallinity of the biocomposites. From the results, it is noticed that TPS only biocomposites are semi-crystalline materials with some degree of crystallinity. However, as nanokaolin is introduced into the TPS matrix, the crystallinity is seen to increase.

From the TGA results, the thermograms showed that there was mass loss in the biocomposites which corresponded to water losses, decomposition of starch, evaporation of glycerol, and somehow the dehydrolisation of the cellulose structure and the silicates of the nanokaolin.

From the DSC results, it is noticed that for biocomposites reinforced with nanokaolin and cellulose, as the volume fraction of the reinforcing material increases, the temperature required to reach the peak occurs at lower temperatures. Also, it is noticed that the energy absorbed reduces as the volume fraction of the reinforcement increases.

From the various analysis techniques and results, it is noticed that all biocomposites fabricated showed promising properties and results.

5.2. Recommendations

1) Various packaging applications should be explored with this composite
2) Further work could be conducted to study the properties of biocomposites fabricated by combining nanokaolin and cellulose nanofibers as modifiers.
3) Further work could be done to investigate the surface roughness of biocomposites fabricated for packaging application.
4) Future work could be conducted to compare the properties of natural material based biocomposites to synthetic material based biocomposites.

5) Future work could be done to investigate the barrier potential of the biocomposite films to oxygen and other gases.

REFERENCES

[1] Abubakar Sandaria, "Eco-Friendly Packaging in Restaurants In Accra-Application , Attitudes And Challenges", Kwame Nkrumah University Of Science And Technology, Kumasi, College Of Science, faculty Of Biosciences, Department Of Food Science And Technology, 2016.

[2] A. Emblem and H. Emblem, "Packaging Technology: Fundamentals, Materials and Processes," Cornwall: Woodhead Publishing Limited, 2012.

[3] A. Mohanty, M. Misra, L. T. Drzal, "Sustainable bio-composites from renewable resources:opportunities and challenges in the green materials world," J Polym Environment, vol. 10, pp. 19-26, 2002.

[4] Anon, available online at: https://education.seattlepi.com/environmental-problems-caused-synthetic-polymers-5991.html accessed 20 Aug. 2018.

[5] A. Peshin, "What is the stress-strain curve?", article viewed on 7th March, 2019, viewed from www.scienceabc.com, 2019.

[6] A. Rafiq and N. Merah, "Nanoclay enhancement of flexural properties and water uptake resistance of GFR epoxy composites at different temperatures," Journal of Composite Materials, 2018.

[7] A. S. Nur Hanani, A. Zuliahani, W. I. Nawawi, N. Razifad, A. R. Rozyanty, " The effect of various acids on the properties of microcrystalline cellulose (MCC) extracted from rice husk (RH)", IOP Conf. series, Materials Science and Engineering, 204, 2017.

[8] A. Sorrentino, G. Gorrasi, V. Vittoria, "Potential perspective of bio-nanocomposites for food packaging applications., Trends Food Science Technology, vol. 18, pp. 84-95, 2007.

[9] ASTM, Annual book of ASTM standards, “Standard test for water vapor transmission of Materials-ASTM E 96-95”, 100 Barr Harbor Drive, West Conshohocken, PA 19428-2959, United States, 1995.

[10] B. A. Adejumo, “Preliminary Investigations on Some Mechanical Properties of Selected Plastic Packaging Materials for Gari Packaging in Nigeria,”International Journal of Scientific & Technology Research, vol. 2, no. 10, ISSN 2277-8616, 2013.

[11] Chemistry LibreTexts, “29.1: There Are Two Major Classes of Synthetic Polymers”, available online at https://chem.libretexts.org/Textbook Maps/Organic Chemistry, accessed 20 Aug. 2018.

[12] Chris DeArmitt, “Functional fillers for plastics”, Applied Plastic Engineering Handbook, William Andrew Publishing, Pg. 455-468, ISBN 9781437735147, 2011.

[13] C. McKown, “Containers. In: Coatings on glass—technology roadmap workshop,” Livermore, Calif: Sandia National Laboratories report, pp. 8–10, 2000.

[14] Council of the European Parliament, “Directive 94/62/EC as regards reducing the consumption of lightweight plastic carrier bags,” 2015, available online at: http://eur-lex.europa.eu/legal-content/EN/TXT/?uri=celex%3A32015L0720, accessed 11th July 2018.

[15] Environmental protection agency (EPA), “Ghana state of environment report 2016”, Ministry of Environment, Science, Technology and Innovation, Accra, 2017.

[16] EU Commission, “Assessment of impacts of options to reduce the use of single use plastic carrier bags,” European Commission-Dg Environment, bio Intelligence Service, 2011, available at: http://ec.europa.eu/environment/waste/packaging/pdf/report-options.pdf, accessed 11th July, 2018.

[17] F.G. Torres, O. P. Trancore, C. Torres, D. A. Diaz, E. Amaya, “Biodegradability and mechanical properties of starch films from Andean corps”, International Journal of Biological Macromolecules, vol. 48, pp. 603-606, 2011.

[18] Fiber products: American fiber manufacturers (2017). Viewed on 16th November, 2018 from www.fibersource.com/fiberproducts.

[19] G. Abood Habeeb and H. Bin Mahmud, “Study on properties of rice husk ask and its use as cement replacement material”, Materials Research, vol. 13, no. 2, 2010.

[20] G. Eckold, “Design and manufacture of composite structures”, Woodhead publishing, 1994.

[21] G. L. Robertson, “Food Packaging: Principles and Practice,” 3rd ed. Boca Raton: Taylor & Francis Group, 2013.

[22] H. Katherine and N. John, “Kenya imposes world's toughest law against plastic bags,” available online at: http://www.reuters.com/article/us-kenya-plastic/kenya-imposes-worlds-toughest-law-against-plastic-bags-idUSKCN1B80NW, accessed 11th July 2017.

[23] J. Hong, X.A Zeng, R. Buckow, Z. Han, M. Wang, “Nanostructure, morphology and functionality of cassava starch after pulsed electric fields assisted acetylation”, Food Hydrocolloids, vol54. Pp 139-150, 2016.

[24] J. N. Hahladakis, Costa A. Velis, Roland Weber, Eleni Lacovidou, Phil Purnell, “An overview of chemical additives present in plastics: Migration, release, fate and environmental impact during their use, disposal and recycling”, Journal of Hazardous Materials, vol. 344, pp.179-199, 2018.

[25] Johannes Schroeter and Marco Hobelsberger, “On the mechanical properties of native starch granules and starch-strong, vol. 44, no.7, pp. 247-252, 1992.

[26] Johar Nurain, Ahmed Ishak, Dufresne Alain, “Extracting and Characterisation of Cellulose fibers and Nanocrystals from rice husk”, Industrial crops and products, vol. 37, pp. 93-99, 2012.

[27] J. Suwanpreteeb and K. Hatthaparit, “Rice-husk-ash based silica as a filler for embedding composites in electronic devices”, Journal of Applied Polymer Sciences, Vol.86, no.12, 2002.

[28] J. W. Rhim, “Effect of clay contents on mechanical and water vapor barrier properties of agar-based nanocomposite films,” Carbohydrate Polymers, vol. 86, pp. 691–699, 2011.

[29] K. L. Yam, P.T. Takhistov, and J. Miltz., “Intelligent Packaging: Concepts and Applications,” Journal of Food Science, vol. 70, no. 1, 2005.

[30] L. Wachowski and L. Domka, “Sources and effects of asbestos and other mineral fibers present in ambient air”, 2010.

[31] L. Yeng and N. Othman, “regenerated cellulose prepared by using NaOH/Urea”, World Academy of Science, Engineering and Technology, International Science, index of materials and metallurgical engineering, vol 8, pp. 12, 2014.

[32] M. Aaron, 2014, “California Plastic Bag Ban Would Be First of Its Kind in The Nation,” available online at: https://www.huffingtonpost.com/entry/californiaplastic-bag-ban_n_5740332.html, accessed 11th July 2018.

[33] M. Al-Qadhi, N. Merah, Z.M Gasem, N. Abu-Dheir, and B.J. Aleem, “ Effect of water and crude oil on mechanical and thermal properties of epoxy-clay nanocomposites”, Polymer Composites, vol. 35, no. 2, pp. 318-326, 2014.

[34] Ma, X., Chang, P.R., Zheng, P., Yu, J. and Ma, X. (2010) Characterization of New Starches Separated from Several Traditional Chinese Medicines. Carbohydrate Polymers, 82, 148-152.

[35] M. Gasper, Z. Benko, G. Dogossy, K. Recsey, T. Gzigany, “Reducing water absorption in compostable starch based plastics”, Polymer Degradation and Stability, vol. 90, pp. 563-569, 2005.

[36] Mineral wool manufacturing-EP, Viewed on 16th November, 2018 from www.epa.gov/ttnchie1/final, 2007.

[37] M. Karamanliohn, P. Richard, D. Robson Geoffrey, “Abiotic and biotic environmental degradation of the bioplastic polymer polylactic acid: a review”, Polymer Degradation and stability, vol. 137, pp 122-130, 2017.

[38] M. Kenneth and B. Betty, “Food Packaging—Roles, Materials, and Environmental Issues,” JOURNAL OF FOOD SCIENCE- Institute of Food Technologists, vol. 72, no. 3, pp. 17750-3841, 2007.

[39] M. Khalique Ahmed, P. Michael McLeod , Jean Nézivar and W. Allison Giuliani, “ Fourier transform infrared and near-infrared spectroscopic methods for the detection of toxic Diethylene Glycol (DEG) contaminant in glycerin based cough syrup”, Spectroscopy vol 24, pp. 601–608, 2010.

[40] M. Maiti, S. Mitra, A.K. Bhowmick, “Effect of nanoclay on high and low temperature degradation of fluoroelastomers”, Polymer Degradation Stability, vol. 93, pp 188-200, 2008.

[41] Mutungi, C., Onyango, C., Doert, T., Paasch, S., Thiele, S., Machill, S., Jaros, D. and Rohm, H. (2011) Long- and Short-Range Structural Changes of Recrystallised Cassava Starch Subjected to in Vitro Digestion. Food Hydrocolloids, 25, 477-485.

[42] M. Wilson, “Clay mineralogical and related characterisics of geophagic materials”, J. Chem. Ecol, vol. 29, pp, 1525-1547, 2003.

[43] M. Zimniewska and A. Kicinska-Jakubowska, “Vegetable fiber sheet. Institute of Natural and Medicinal Plants”, 2012.

[44] N. B Colthup, Daly L. H, Wiberly S.E, “Introduction to infrared and Raman spectroscopy”, Academic Press, New York, 1975.

[45] N. Farmer, “Trends in packaging of food, beverages and other fast- moving consumer goods,” Cambridge: Woodhead Publishing Limited, 2013.

[46] N. Hassan and Mohsen Mosadegh, “Preparation and Properties of Starch/Nanosilicate Layer/Polycaprolactone Composites”, Journal of Polymers and the Environment, vol. 19, pp. 980-987, 2011.

[47] N. H. Mondol, J. Jens and B. Knut, “Elastic properties of clay minerals”, The leading Edge, 2018.

[48] N. Pedro, R. Marim, G. Carvalho and M. Suzana, “Nanocellulose Produced from Rice Hulls and its Effect on the Properties of Biodegradable Starch Films”, Materials Research, vol.10, pp. 1980-5373, 2015.

[49] N. R. Savadekar, V.S Karande, N. Vigneshwaran, A. K. Bharimalla and S.T. Mhaske, “Preparation of nano cellulose fibers and its application in kappa-carrageenan based film”, International Journal of biological macromolecules, no. 51, pp. 1008-1013, 2012.

[50] N. Yalcin and V. Sevinc, “Studies on silica obtained from rice husk”, Ceramics International, vol. 27, pp. 219-224, 2001.

[51] Petra, “About PET,” 2015, available online at: http://www.petresin.org/aboutpet.asp, accessed 10th July, 2018.

[52] P. K. Dutta, S. Tripathi., G.K. Mehrotra and J. Dutta, “Perspectives for chitosan based anti-microbial films in food applications,” Food Chem., vol. 114, pp. 1173-1182, 2009.

[53] Polyprint.com, Poly Print: Water Vapor Transmission Rate, available online at www.polyprint.com/flexograpghic-wvtr.htm, accessed 15th January, 2019.

[54] P. R Griffith, de Haseth J. A, “Fourier transform infrared spectroscopy”, Wiley, New York, 1986.

[55] R. Coles and M. Kirwan, “Food and Beverage Packaging Technology,” 2nd ed. New Delhi: Blackwell Publishing Ltd., 2011.

[56] R. J. Roberts, P.York, “The poisson’s ratio of microcrystalline cellulose”, International journals of pharmaceutics, vol. 105, pp. 177-180, 1994.

[57] R. Mao and Ton Peijs, “Modelling the elastic properties of cellulose nanopaper”, Materials and Design, vol. 126, pp. 183-189, 2017.

[58] R. Quashie and J. Carruthers, “Technology overview: Bionanocomposites”, Knowlegde Transfer Networks, netcomposites, 2014.

[59] R. Suryana, Y. Iriani, F. Nurosyid and D. Fasquelle, “Characteristics of silica rice husk ash from Mojogedang Karanganyar Indonesia”, IOP Conference: Materials Science and Engineering, no.367, 2018.

[60] Rtilab, “Techniques-FTIR Analysis”, Environmental, chemical and Materials testing labouratory, 2015, accessed from www.rtilab.com, accessed on 28th December, 2018.

[61] S. Joongmin and S. E. M. Susan, “Food Processing: Principles and Applications,” John Wiley & Sons, Ltd. Published 2014 by John Wiley & Sons, Ltd, 2014.

[62] S. k. Shukla, Saga Naman, deepika Sundram, Prateeksha Ankur, Arun Srishti, Vaishali Rakesh, A. Bharadvaja and G. C. Dubey, “Extraction of cellulose micro sheets from rice husk: a scalable chemical approach”, DU Journal of undergraduate research and innovations, vol. 1, issue 3, pp. 187-184, 2015.

[63] S. Ray, A. Eastral, S.Y. Quek, X.D. Chen, “The potential use of polymer clay nanocomposites in food packaging”, International Journal of Food Engineering, vol. 2, pp 1556-3758, 2006.

[64] S. Sacharow and R. C. Griffin, “The evolution of food packaging,” Principles of food packaging, 2nd ed. Westport, Conn.: AVI Publishing Co. Inc. pp. 1–61, 1980.

[65] S. Zuzana, “Food Packaging Materials Comparison of Materials Used for Packaging Purposes,” Helsinki Metropolia University of Applied Sciences, 2017.

[66] T. Guzman Jon, S. Peter, D. Egede Anders, H. Ole,” Hybrid nanocellulose/nanoclay composites for food packaging applications,” Kgs Lyngby: Danmarks Tekniske Universitet, 2016.

[67] V. D Alves, S. Mali, A. Beleia, M.V.E Grossmann, “Effect of glycerol and amylose enrichment on cassava starch film properties”, Journal of food engineering, vol.78, pp 941-946, 2007.

[68] W. Affo, N. Y. Samuel, R. Amponsah, J.K. Efavi, “Development of cassava bioplastics for consumer packaging”, Journal of Ghana Science Association, Vol 14, No. 2, 2012.

[69] W. D. Callister, “Materials Science and Engineering: an introduction”, 7th edition, USA: John Wiley and Sons Inc., Pg. 580-581, 595, 2007

[70] Whatisengineering, “Abaqus”, viewed from whatisengineering.com/topic/abaqus, viewed on 17th November, 2018, 2016.

[71] W. Soboyejo, “Mechanical Properties of Engineered Materials”, Princeton University, New Jersey, Mercel Dekker Inc., 2003.

[72] W. Soroka, “Packaging functions: fundamentals of Packaging Technology,” Naperville, IL: Institute of Packaging Professionals, pp. 29–48, 2008.

[73] Y. Chen, X. Cao, P.R Chang and M.A Huneault, “Comparative study on the films of Poly (vinyl alcohol)/Pea starch Nanocrystals and Poly(vinyl alcohol)/Native pea starch”, Carbohydrate Polymers, Vol. 73, pp. 8-17, 2008.

[74] Y. Zhang, C. Rempel, Q. Liu, “Thermoplastic starch processing and characteristic-a review”, Crit. Rev. Food Sci. Nutri, vol. 54, no.10, pp.1353-1370, 2014.